LA-UR- 09-00821

Approved for public release;
distribution is unlimited.

Title:	Pentavalent Uranium Chemistry – Synthetic Pursuit of a Rare Oxidation State
Author(s):	Christopher R. Graves and Jaqueline L. Kiplinger*
Intended for:	Chemical Communications

Los Alamos
NATIONAL LABORATORY
EST. 1943

Form 836 (7/06)

Pentavalent Uranium Chemistry – Synthetic Pursuit of a Rare Oxidation State

Christopher R. Graves and Jaqueline L. Kiplinger*

Received (in XXX, XXX) Xth XXXXXXXXX 200X, Accepted Xth XXXXXXXXX 200X
First published on the web Xth XXXXXXXXX 200X
DOI: 10.1039/b000000x

This Feature Article presents a comprehensive overview of stable pentavalent uranium systems in non-aqueous solution with a focus on the various synthetic avenues employed to access this unusual and very important oxidation state. Selected characterization data and theoretical aspects are also included. The purpose is to provide a perspective on this rapidly evolving field and identify new possibilities for the future development of pentavalent uranium chemistry.

Introduction

Although uranium has various oxidation states (III, IV, V, VI) in both solution and the solid-state, the trivalent, tetravalent and hexavalent complexes have dominated the landscape of uranium chemistry, with the corresponding pentavalent systems remaining comparatively rare.[1] Historically, this deficit has been attributed to the instability of pentavalent uranium toward redox disproportionation in aqueous solutionto produce the more stable oxidation states U^{IV} and U^{VI}.[2] This instability also reflects the extreme air and water sensitivity of pentavalent uranium and its easy conversion/oxidation to hexavalent uranium in the presence of trace amounts of oxygen or water. Generally speaking, aside from classical coordination complexes of the halides such as UOX_5^{2-}, UX_5 and UX_6^- (X = halide), rational synthetic schemes were simply unknown and the few reported molecular U^V systems came from serendipitous discoveries that were not reproducible. As a consquence, very little was known about pentavalent uranium; most of our existing knowledge about the physicochemical properties associated with this oxidation state has come from halide coordination complexes and was captured in the last comprehensive review on uranium(V) in 1969.[2]

In recent years, the ability to access U^V systems has become more prevalent. Techniques for handling and characterizing air- and water-sensitive materials have vastly improved, enabling a variety of new approaches for synthesizing pentavalent uranium compounds. In fact, in what can only be described as a renaissance in research activity in the field over the past few years, uranium(V) has been shown to be far more stable than previously thought, and its chemistry is important in understanding the behavior of actinides in the environment, corrosion, waste, the nuclear fuel cycle and long-term storage of spent nuclear fuel.[3-8] For example, this once discounted uranium oxidation state has been implicated in the low–temperature chemistry of uranium in reducing, heterogeneous aqueous systems,[9] the biogeochemical reduction of uranium in the environment[10,11] and the immobilization of actinides in aquifers.[12]

These single-electron systems provide fertile ground for not only advancing theoretical capabilities but also our fundamental understanding of actinide electronic structure, reactivity and bonding. For example, because electron repulsion is absent and at most six transitions are allowed in the optical spectrum, the f^1 electronic configuration facilitates the interpretation of spectrosopic[13] and magnetic[14] data. This enables electron paramagnetic resonance (EPR) studies and magnetic susceptibility measurements on systems that promote the formation of Kramers doublet ground states.[2] Additionally, convergence difficulties in Density Functional Theory (DFT) calculations can occur for actinide complexes with unpaired electrons; however, the f^1 electronic configuration in U^V minimizes these problems compared to systems in lower oxidation states (i.e. f^2, f^3).[15] Combined, these techniques provide important insight into 5f element electronic structure and how it manifests itself physically in molecular solution and solid-state structure, as well as chemically through its influence on spectroscopic and thermodynamic properties.

As stated in the title, this Feature Article will describe the field of pentavalent uranium molecular chemistry from 1969 until January 2009, with a primary focus on the synthetic routes to these systems and their structural characterization.† It is broken into three main sections: (1) Pentavalent Uranyl (UO_2^+) Chemistry, (2) Pentavalent Uranium Alkoxide and Amide Systems, and (3) Organometallic Complexes of Pentavalent Uranium. When appropriate, selected details of additional physical characterization or theoretical studies of these systems will also be presented. The early chemistry of U^V-halide and -alkoxide complexes, which was addressed in the 1969 review by Selbin and Ortego,[2] and later by Ryan in 1971,[16] will not be re-covered here. Furthermore, this review will not discuss U^V in extended oxide solids which can be found elsewhere.[17-19]

Pentavalent Uranyl (UO_2^+) Chemistry

Despite the immense body of work devoted to uranyl chemistry, routes for the synthesis of pentavalent uranyl (UO_2^+) systems are lacking compared to their hexavalent equivalents (UO_2^{2+}). This has been proposed to be due to the inherent instability of the UO_2^+ ion toward disproportionation to the more stable UO_2^{2+} and U^{4+} ions (eq. 1).[20-24] However, over the past few years systems with stable pentavalent uranyl

UO_2^+ ions have emerged, which will be reviewed here.‡

$$2\,UO_2^+ + 4\,H^+ \longrightarrow UO_2^{2+} + U^{4+} + 2\,H_2O \quad (1)$$

Synthesis and Characterization of UO_2^+ Complexes in Solution

Pioneering work in the field of pentavalent uranyl chemistry was carried out by Miyake and co-workers concerning the detection of the UO_2^+ ion in solution. Electron paramagnetic resonance (EPR) spectroscopy was used to measure the products of the photo- and electrolytic reduction of the complexes $U^{VI}O_2(L)_n(ClO_4)_2$ (L = dimethylformamide (DMF) (**1**), dimethylsulfoxide (DMSO) (**2**), triethylphosphate (TEP) (**3**)) and $U^{VI}O_2(L)_n(NO_3)_2$ (L = DMF (**4**), DMSO (**5**), TEP (**6**).[25,26] The optical spectra measured in the reductions of these complexes indicated the formation of uranium(V) with λ_{max} at 770, 970 and 1400 nm. Interestingly, both the photo- and electrolytic reduction of the perchlorate systems resulted in a nearly isotopic EPR signal with $g_\perp = 2.5$, while the signal observed for the nitrate complexes varied with reduction technique – electrolytic reduction gave results analogous to the perchlorate complexes and photoreduction afforded an asymmetric signal with $g_\perp = 1.97$. These data reflect differences between the perchlorate and nitrate complexes in the first coordination spheres, with the larger $g_\perp$ value revealing tighter ligand coordination in the equatorial plane than in the axial direction.

Ikeda and co-workers have shown that the hexavalent uranyl carbonate anion $[(U^{VI}O_2)(CO_3)_3]^{4-}$ (**7**) could be quasi-reversibly reduced to the U^V equivalent.[27] They later showed using ^{13}C NMR spectroscopy that the uranyl(V) carbonate complex was $[U^VO_2(CO_3)_3]^{5-}$ (**8**) and that CO_3^{2-} exchange under basic conditions occurs by a dissociative mechanism.[28] It was postulated that incorporation of multidentate ligands in the equatorial sites of the uranyl ion would stabilize the U^V complex upon reduction. Indeed, the $U^{VI}O_2(acac)_2(DMSO)$ (acac = acetylacetonate) (**9**) complex was shown to have quasi-reversible electrochemical behavior in which rapid formation of the neutral $U^VO_2(acac)(DMSO)$ (**10**) complex occurs through initial electron transfer followed by ligand dissociation.[29] Similar quasi-reversible reduction chemistry was observed in the electrochemical analysis of other uranyl complexes possessing bidentate ligand systems such as $U^{VI}O_2(trop)_2(DMSO)$ (trop = tropolonate) (**11**), $U^{VI}O_2(\beta$-diketonato$)_2(DMSO)$ (β-diketonato = benzoylacetonate (ba) (**12**), benzoyltrifluoroacetonate (dtfa) (**13**), thenoyltrifluoroacetonate (ttfa) (**14**)), $U^{VI}O_2(sap)(DMSO)_2$ (sap = 2-salicylidenaminophenolate) (**15**), and $U^{VI}O_2(salen)(L)$ (salen = *N,N'*-disalicylidenethylenediaminate) (**16**) although the mechanism of electron transfer is specific to each case.[30] A summary of the electrochemical data for these systems is presented in Table 1.

Ikeda and co-workers have also prepared the $U^{VI}O_2(saloph)(DMSO)$ (saloph = *N,N'*-disalicylidene-*o*-phenylenediaminate) (**17**) complex and showed that the corresponding pentavalent system can be generated electrochemically.[31] Along with this electrochemical analysis, Ikeda reported the electronic spectra for the species formed by bulk electrolysis of **17**. Absorption bands in the visible-near-infrared (NIR) region (~650, 750, 900, 1400, and 1875 cm^{-1}) were observed with molar extinction coefficents (ε) of 150-900 $M^{-1}cm^{-1}$, characteristic of a U^V species.[32] It was further shown with IR measurements that the U-O bond strength in the $UO_2(saloph)(DMSO)$ complex is weakened upon reduction of UO_2^{2+} to UO_2^+.[33]

Table 1 Electrochemical data for uranyl complexes of the type $UO_2(L)_n(DMSO)_m$ in DMSO.

Complex	E^0 (U^{VI}/U^V)[a]	Mechanism
$UO_2(acac)_2(DMSO)$ (**9**)	-1.44	EC[b]
$UO_2(trop)_2(DMSO)$ (**11**)	-1.379	EC
$UO_2(ba)_2(DMSO)$ (**12**)	-1.416	EC
$UO_2(btfa)_2(DMSO)$ (**13**)	-1.073	E[c]
$UO_2(ttfa)_2(DMSO)$ (**14**)	-1.082	E
$UO_2(sap)(DMSO)_2$ (**15**)	-1.500	EC
$UO_2(salen)(DMSO)$ (**16**)	-1.602	E
$UO_2(saloph)(DMSO)$ (**17**)	-1.550	E

[a]At 25 ± 1 °C versus $[(C_5H_5)_2Fe]^{+/0}$. [b]EC: Mechanism in which a chemical reaction involving the product occurs after electron transfer. [c]E: Mechanism that proceeds through electron transfer at the electrode surface.

Well-Defined Molecular UO_2^+ Complexes

A serendipitous discovery by the Berthet and collaborators provided the first isolated and structurally characterized uranyl(V) system.[34] During the course of studying the synthesis and structure of anhydrous uranyl triflate complexes, crystals of $[U^VO_2(O{=}PPh_3)_4][OSO_2CF_3]$ (**18**) were isolated.[34]

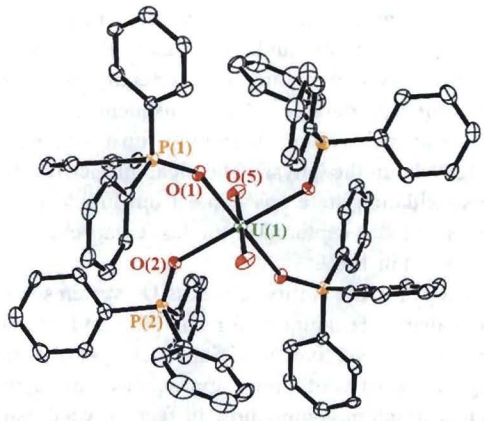

Figure 1 Molecular structure of the $[U^VO_2(O{=}PPh_3)_4]^+$ cation in complex **18**.

The $[U^VO_2(O{=}PPh_3)_4]^+$ cation features a square bipyramidal configuration at the metal center with a linear uranyl subunit (Figure 1). The $U{=}O_{uranyl}$ distances found for the two independent $[U^VO_2(O{=}PPh_3)_4]^+$ ions in the unit cell (1.817(6), 1821(6) Å) are 0.06 Å longer than their counterparts (1.7632(16), 1.7603(15) Å) in the hexavalent $[U^{VI}O_2(O{=}PPh_3)_4][OSO_2CF_3]_2$ complex (**19**).[34] This lengthening of the $U{=}O_{uranyl}$ bonds is in accord with theoretical calculations[35] performed on $[UO_2(H_2O)_5]^{n+}$ and X-ray absorption fine structure (EXAFS) studies carried out on the $[U^{VI}O_2(CO_3)_3]^{4-} \rightarrow [U^VO_2(CO_3)_3]^{5-}$ reduction, which

showed minor geometrical rearrangements between the two species.[36] Attempts to reduce $[U^{VI}O_2(O{=}PPh_3)_4][OSO_2CF_3]_2$ (**19**) either photochemically or using various reducing agents to access **18** were not successful.[34]

Systems similar to those studied by Ikeda have recently been examined by the Hayton group who demonstrated that the $[U^{V}O_2]^+$ moiety can be kinetically stabilized by ligand sets, which provide steric bulk in both the uranyl equatorial plane and along the O=U=O axis.[37] Reduction of the uranyl(VI) species $[U^{VI}O_2(Ar_2nacnac)(O{=}PPh_2Me)_2][OSO_2CF_3]$ (**20**) ($Ar_2nacnac$ = bis(2,6-diisopropylphenyl)pentane-2,4-di-iminato) with cobaltocene ($(C_5H_5)_2Co$) provides the neutral uranyl(V) complex $U^{V}O_2(Ar_2nacnac)(O{=}PPh_2Me)_2$ (**21**) in good (74%) isolated yield (eq. 2) Although stable at -25 °C, this complex proved to be reactive and was readily oxidized back to the starting material with AgOTf.

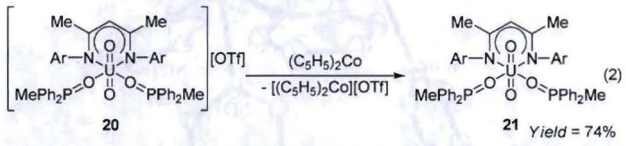

Complex **21** was characterized crystallographically (Figure 2) and exists in a distorted octahedral geometry with a *trans* (O(1)-U(1)-O(2) = 178.4(2)°) uranyl unit. Again, the $U{=}O_{uranyl}$ distances in $U^{V}O_2(Ar_2nacnac)(O{=}PPh_2Me)_2$ (1.810(4), 1.828(4) Å) were found to be slightly longer than those observed for the U^{VI} cation in **20** (1.756(4), 1.748(4) Å). Supporting evidence for a weaking of the $U{=}O_{uranyl}$ bonds in $U^{V}O_2(Ar_2nacnac)(O{=}PPh_2Me)_2$ relative to $[U^{VI}O_2(Ar_2nacnac)(O{=}PPh_2Me)_2]^+$ came from IR spectroscopy; the asymmetric stretch for $U^{V}O_2(Ar_2nacnac)(O{=}PPh_2Me)_2$ appears at 800 cm^{-1}, while that for $[U^{VI}O_2(Ar_2nacnac)(O{=}PPh_2Me)_2]^+$ lies at higher enegy (918 cm^{-1}).[37] Such a shift is in agreement with the results found for Ikeda's $U^{V}O_2$(saloph)(DMSO) system.[33]

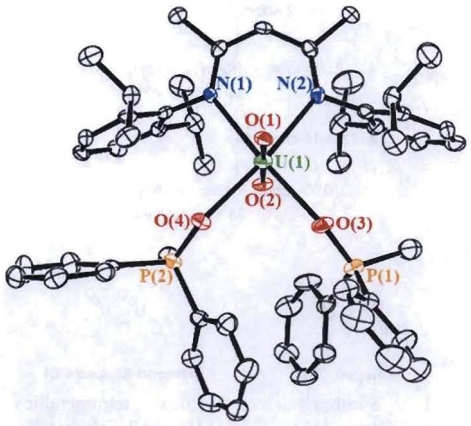

Figure 2 Molecular structure of $U^{V}O_2(Ar_2nacnac)(O{=}PPh_2Me)_2$ (**21**).

Hayton and co-workers have also examined the chemistry of β-diketiminate/β-diketonate uranyl complexes of the type $UO_2(Ar_2nacnac)(RC(O)CHC(O)R)$ ($Ar_2nacnac$ = bis(2,6-diisopropylphenyl)pentane-2,4-di-iminato; R = Me, Ph, CF_3).[38] Electrochemical analysis of the U^{VI} complexes showed that there was a systematic decrease in the U^{VI}/U^{V} reduction potentials with variation of the R group in the β-diketonate ligand (R = Me (**22**), U^{VI}/U^{V} = -1.82 V; R = Ph (**23**), U^{VI}/U^{V} = -1.59 V; R = CF_3 (**24**), U^{VI}/U^{V} = -1.39 V, all versus $[(C_5H_5)_2Fe]^{+/0}$). This trend tracks with the electronic donating ability of the ligand, such that the more electron withdrawing ligand (R = CF_3) affords a more electron poor and easily reduced uranium center. This difference in potential is also manifested in the chemical reduction of the complexes **22-24**. While $U^{VI}O_2(Ar_2nacnac)(CF_3C(O)CHC(O)CF_3)$ (**24**) was readily reduced to the anion $[U^{V}O_2(Ar_2nacnac)(CF_3C(O)CHC(O)CF_3)]^-$ using $(C_5H_5)_2Co$, the more reducing decamethylcobaltocene $[(C_5Me_5)_2Co]$ was required for the reduction of $U^{VI}O_2(Ar_2nacnac)$(MeC(O)CHC(O)Me) (**22**) and $U^{VI}O_2(Ar_2nacnac)$(PhC(O)CHC(O)Ph) (**23**) (eq. 3). The resultant reduction products were discrete cation/anion pairs: $[(C_5R'_5)_2Co][U^{V}O_2(Ar_2nacnac)(RC(O)CHC(O)R)]$ (**25-27**).

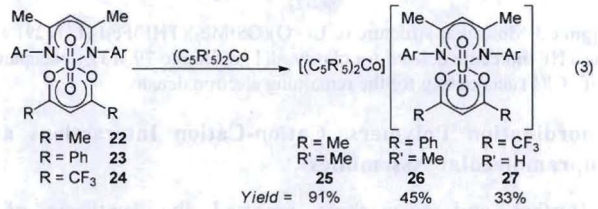

Recently, Arnold, Love and co-workers reported the selective reductive silylation of the *exo*-U=O moiety in the macrocyclic complex **28** to produce the complex $U(=O)(OSiMe_3)(THF)Fe_2I_2(L^1)$ (**29**), where L^1 represents the multidentate macrocycle ligand.[39] The authors propose that initial double deprotonation of the lower cavity in complex **28** affords an activated U^{VI} intermediate in which the *endo*-U=O bond is coordinated by two K^+ ions. This enables sufficient polarization of the *exo*-U=O bond, resulting in N-Si cleavage from either the by-product $H{-}N(SiMe_3)_2$ or $N(SiMe_3)_3$. Metallation with FeI_2 gives complex **29** in 80% yield (eq. 4). Such a mechanistic pathway has been supported by DFT calculations.[40]

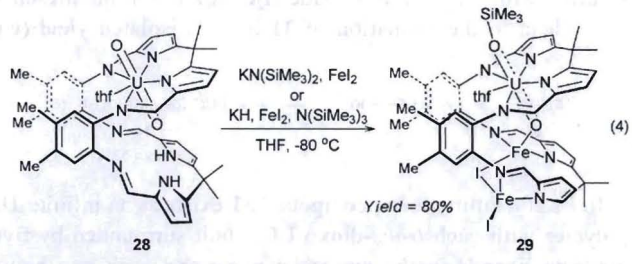

The uranium metal center in **29** features a distorted pentagonal bipyramid geometry with the $SiMe_3$ group being bound to the *exo*-uranyl oxygen, while the *endo*-uranyl oxygen forms a dative bond to one of the iron atoms in the lower wedge of the macrocycle (Figure 3). The uranyl unit in this U^{V} complex maintains linearity (O(1)-U(1)-O(2) = 172.16(17)°), although there is a marked difference in the U-O_{uranyl} bond lengths: the *endo* distance (U(1)-O(1) = 1.870(4)

Å) is significantly shorter than the corresponding *exo* parameters (U(1)-O(2) = 1.993(4) Å). It is noteworthy to point out that the U(1)-O(2) distance is still shorter than U-O distances found in other structurally characterized U-OSiMe$_3$ complexes,[41] indicating that the *exo*-uranyl in complex **29** retains some multiple bond character.

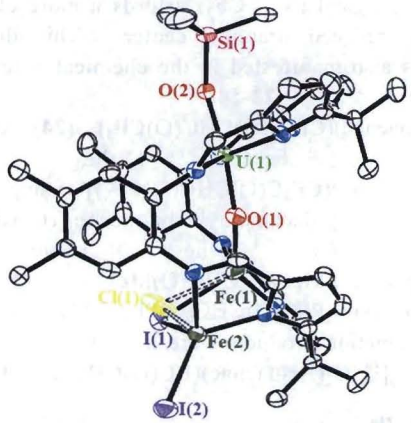

Figure 3 Molecular structure of U(=O)(OSiMe$_3$)(THF)Fe$_2$I$_2$(L^1) (**29**) with the THF molecule deleted for clarity. I(1) refines to 79.7(3)% occupancy, with Cl(1) accounting for the remaining electron density.

Coordination Polymers, Cation-Cation Interactions and Supramolecular Assemblies

Berthet and co-workers reported the synthesis of a polymeric pentavalent uranyl compound $\{[U^VO_2(py)_5][KI_2(py)_2]\}_\infty$ (**31**).[42] A 1:1 reaction between $UO_2I_2(THF)_3$ (**30**) and KC_5Me_5 in pyridine (py) provides **31**, which under dynamic vacuum gives $U^VO_2(py)_{2.2}I_2K$ (**32**) in 80% isolated yield (eq. 5).

$$\underset{\mathbf{30}}{UO_2I_2(THF)_3} + KC_5Me_5 \xrightarrow[-1/2\ (C_5Me_5)_2]{py} \underset{\mathbf{31}}{\{[UO_2(py)_5][KI_2(py)_2]\}_\infty} \xrightarrow{vac} \underset{\mathbf{32}}{UO_2(py)_{2.2}I_2K} \quad (5)$$

Yield = 80%

In a contemporary report by the Mazzanti group, the identical U^V polymer was prepared using oxidation chemistry rather than the reductive protocol employed by Berthet. The controlled 2-electron oxidation of $UI_3(THF)_4$ (**33**) in pyridine solution with a pyridine *N*-oxide/H_2O mixture in the presence of KI lead to the formation of **31** in 53% isolated yield (eq. 6).[43]

$$\underset{\mathbf{33}}{UI_3(THF)_4} + \text{py-O/H}_2\text{O} + KI \longrightarrow \underset{\mathbf{31}}{\{[UO_2(py)_5][KI_2(py)_2]\}_\infty} \quad (6)$$

Yield = 53%

In its crystalline form, compound **31** exists as an infinite 1D polymer with each *trans*-dioxo UO_2^+ unit surrounded by five pyridine ligands in the equitorial plane and each oxo being capped by an anionic $[KI_2(py)_2]^-$ fragment. The polymeric nature of this material results from the ability of the UO_2^+ fragments to form cation-cation interactions (CCIs) through the highly basic uranyl oxygens.[42,43] The molecular structure of the repeating unit in **31** is shown in Figure 4.

The magnetic response of **31** was measured and an effective magnetic moment (μ_{eff}) of 2.57 μ_B/U at 300 K was observed,[44] which is close to the theoretical value of 2.54 μ_B/U calculated for the free 5f^1 ion in the L-S coupling scheme.[45] A plot of the χT product versus T shows two distinct temperature regimes. The high temperature (~50-300 K) regime is linear with a large slope, while the χT product rapidly decreases in the low temperature (2-~50 K) region. This magnetic behavior is consistent with that seen for the simple UV-halide coordination complexes,[2] and suggests the presence of localized 5f^1 ions in the polymer network. Evidence for magnetic coupling between the U^V ions in **31** was not seen in a plot of χ versus T.

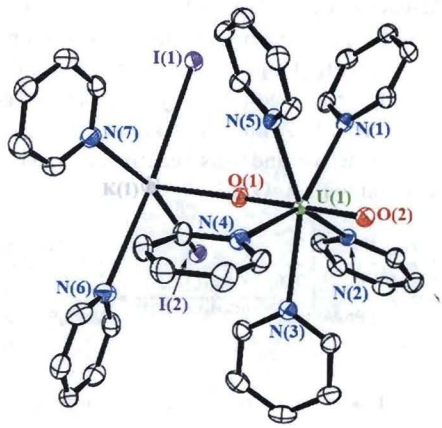

Figure 4 Molecular structure of the repeating unit in the $\{[U^VO_2(py)_5][KI_2(py)_2]\}_\infty$ (**31**) coordination polymer.

The Mazzanti group further utilized CCIs to construct uranyl(V) supramolecular assemblies. Reaction between $\{[U^VO_2(py)_5][KI_2(py)_2]\}_\infty$ (**31**) and 2 equiv. Kdbm (dbm$^-$ = dibenzoylmethanate) affords the tetrametallic complex $\{[U^VO_2(dbm)_2]_4[K_6(py)_{10}]\}I_2(py)_2$ (**34**) in 70% yield. Further reaction of **34** with excess 18-crown-6 provided the bimetallic complex $[U^VO_2(dbm)_2K(18\text{-crown-}6)]_2$ (**35**) in 45% yield (Scheme 1).[44,46]

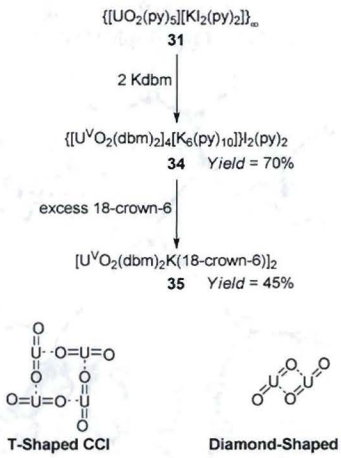

Scheme 1 Synthesis of the tetrametallic complex $\{[U^VO_2(dbm)_2]_4[K_6(py)_{10}]\}I_2(py)_2$ (**34**) and bimetallic complex $[U^VO_2(dbm)_2K(18\text{-crown-}6)]_2$ (**35**).

The cation in complex **34** exists as a centrosymmetric tetramer of UO_2^+ ions coordinated to each other in a monodentate fashion. Each UO_2^+ coordinates to two adjacent uranyl groups using two T-shaped cation-cation interactions. Each UO_2^+ is also involved in a CCI with a potassium ion

(Figure 5).[44,46] CCIs have been implicated in the aqueous disproportionation reaction of uranyl(V) to uranium(IV) and uranyl(VI) species and recent theoretical studies have suggested that this disproportionation proceeds through dimeric T-shaped CCIs.[24] Solution studies carried out on complex **34** support these proposals.

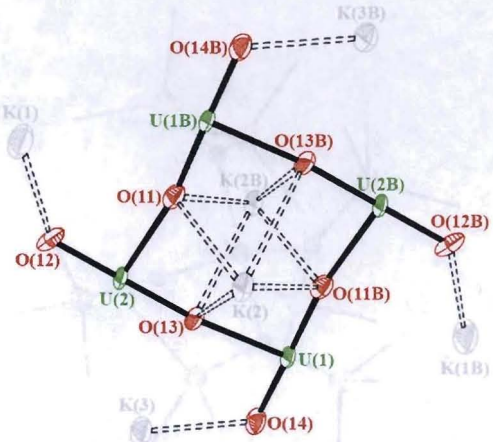

Figure 5 Molecular structure of the tetramer core of uranyls in the $\{[U^{V}O_2(dbm)_2]_4[K_6(py)_{10}]\}I_2(py)_2$ (**34**) complex with the pyridine, iodide and dbm ligands omitted for clarity.

Complex **35** was found to exist as a centrosymmetric dimer in which two $[UO_2(dbm)_2]^-$ units are assembled in a diamond shaped CCI (Figure 6).[44] Unlike the 1D polymer **31**, the magnetic behavior of **35** clearly shows the presence of antiferromagnetic coupling between the U^{V} ions, which is proposed to occur through a superexchange mechanism, with a maximum in χ versus T at ~5K. A μ_{eff} of 1.69 μ_B/U at 300 K was observed. The solid-state magnetic data for the tetrameric complex $\{[UO_2(dbm)_2]_2[\mu\text{-}K(N{\equiv}C\text{-}CH_3)_2(\mu_8\text{-}K)]\}_2$ (**36**) also suggested magnetic coupling, albeit at lower temperatures. The dissimilar magnetic behavior between **35** and **36** was ascribed to the different geometric arrangement of the interacting uranyl(V) groups.

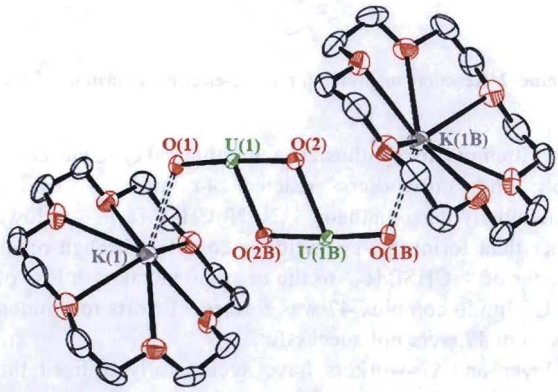

Figure 6 Molecular structure of the diamond shaped core of uranyls in the $[U^{V}O_2(dbm)_2K(18\text{-crown-}6)]_2$ complex (**35**). The dbm ligands have been omitted for clarity.

Recently, Boncella and co-workers reported the synthesis of an imido variant of the uranyl cation $[U^{V}(=N\text{-}^{t}Bu)_2I(^{t}Bu_2bpy)]_2$ (**38**) ($^{t}Bu_2bpy$ = 4,4′-di-tert-butyl-2,2′-bipyridyl), which was formed in 72% yield utilizing synthetic chemistry similar to that employed by Berthet in the synthesis **31**. Formal reduction of the hexavalent complex $U(=N\text{-}^{t}Bu)_2I_2(^{t}Bu_2bpy)$ (**37**) in its reaction with 2 equiv. of $Na(C_5Me_5)$ (eq. 7).[47] In the solid-state, complex **38** exists as a dimer with the two $[U(=NR)_2]^+$ units engaged in cation-cation interactions (Figure 7). This is the first example of a structurally characterized pentavalent bis(imido) uranium(V) ion. As with complex **35**, the χ versus T magnetic data collected for **38** clearly shows the presence of an antiferromagnetic coupling interaction between the two $5f^1$ ions with a maximum at ~13 K. A μ_{eff} of 1.48 μ_B/U at 300 K was observed.

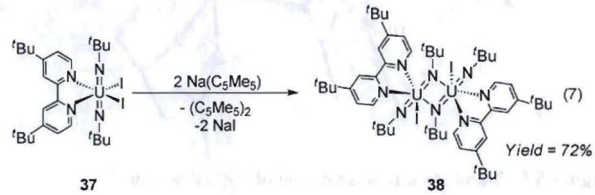

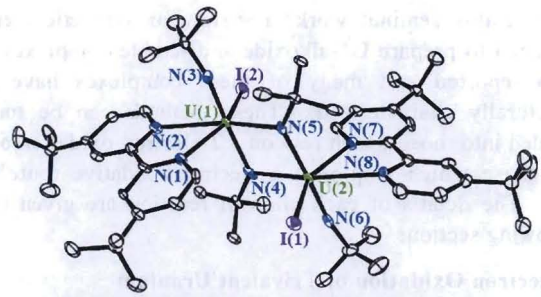

Figure 7 Molecular structure of $[U^{V}(=N\text{-}^{t}Bu)_2I(^{t}Bu_2bpy)]_2$ (**38**).

Pentavalent Uranium Alkoxide and Amide Systems

Alkoxide, halide alkoxide and oxo halide compounds have traditionally dominated the field of pentavalent uranium chemistry, and Selbin and Ortego give a detailed account of the chemistry and physicochemical properties of these classes of compounds up until 1969.[2] The following sections of this review provide an update regarding the chemistry of uranium(V) alkoxide and amide complexes.

Early Work – Solution Studies and the First Structure

Despite the extensive early chemistry of the U^{V} alkoxides, historically they represented an under-characterized group of compounds, with little known about their physical and chemical properties. In the early 1980's, the Eller group reported the low-temperature (-65 °C) ^{1}H NMR of $U(OEt)_5$ (**39**).[48] They observed a four-line pattern consistent with a dimeric structure containing edge-bridging octahedra with bridging ethoxide units, which are magnetically inequivalent with the terminal ethoxide ligands. The Cotton group reported the first structural characterization of a pentavalent uranium alkoxide complex (Figure 8).[49,50] The $[U(O^{i}Pr)_5]_2$ (**40**) complex is a dimer, which agrees with the ^{1}H NMR findings described by Eller for the related uranium ethoxide complex. The dimer resides on an inversion center and presents an edge-sharing bioctahedral geometry with a U···U distance of 3.789(1) Å. The terminal U-O distances (2.03(1)

Å) are slightly shorter than the bridging U-O distances (2.29(1) Å). Subsequent theoretical studies by Bursten and co-workers showed that the strong alkoxide π–donor ligands in the edge-sharing bioctahedral geometry of **40** overpowers the $5f^1$-$5f^1$ interactions that are needed to form a U-U bond.[51]

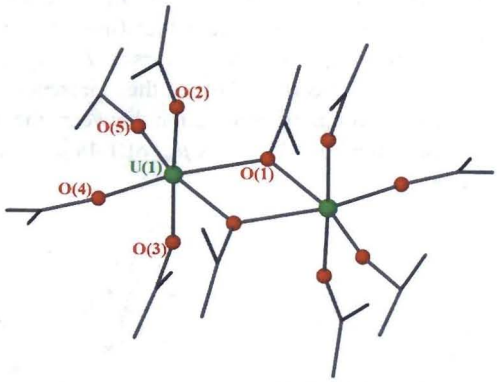

Figure 8 Ball-and-stick representation of $U_2(O^iPr)_{10}$ (**40**).

Since this seminal work, a variety of synthetic methods designed to prepare U^V-alkoxide and -amide complexes have been reported and many of these complexes have been structurally characterized. These methods can be roughly divided into those which rely on a 2-electron oxidation of U^{III} and those which employ a 1-electron oxidative route from U^{IV}. The details of each class of reaction are given in the following sections.

2-Electron Oxidation of Trivalent Uranium

The reaction of trivalent uranium with 2-electron oxidizing agents has proven to be a reliable route for the generation of pentavalent uranium compounds. Andersen and co-workers first showed that reaction between the tris(amido) complex $[N(SiMe_3)_2]_3U$ (**41**) and 1 equiv. of trimethylamine-*N*-oxide yielded the U^V-oxo complex $[N(SiMe_3)_2]_3U(=O)$ (**42**) in 50% yield (eq. 8).[52] The Andersen group went on to show that the corresponding imido complex $[N(SiMe_3)_2]_3U(=N\text{-}SiMe_3)$ (**43**) could be formed in a similar manner from the reaction between **41** and 1 equiv. of TMS-azide ($N{=}N{=}N\text{-}SiMe_3$) at room temperature (eq. 9).[53]

$$[N(SiMe_3)_2]_3U \xrightarrow[-\ NMe_3]{Me_3N^+\text{-}O^-} (Me_3Si)_2N\text{–}U(=O)\text{–}N(SiMe_3)_2 \quad (8)$$

41 **42**

$$[N(SiMe_3)_2]_3U \xrightarrow[-\ N_2]{+\ N{=}N{=}N\text{-}SiMe_3} (Me_3Si)_2N\text{–}U(=N\text{–}SiMe_3)\text{–}N(SiMe_3)_2 \quad (9)$$

41 **43**

In the solid-state, compound **43** exists in a *pseudo*-tetrahedral geometry with the three $N(SiMe_3)_2$ groups sitting on a 3-fold axis. A short $U{=}N_{imido}$ bond distance (U(1)-N(1) = 1.91(2) Å) and linear U=N-Si angle (U(1)-N(1)-Si(1) = 180.00°) are hallmarks of this pentavalent imido complex (Figure 9). Together, these data suggest that both lone pairs of the nitrogen atom are bonding to the uranium, creating a $U{=}N_{imido}$ linkage that is best viewed as a triple bond.

Similar chemistry has been used by the Scott group to synthesize a variety of U^V complexes of the type $(NN'_3)U{=}E$, where $NN'_3 = N(CH_2CH_2NSiMe_2{}^tBu)_3$ and E represents an imido or oxo functional group.[54] Reaction of the trivalent starting complex **44** with 1 equiv. $N{=}N{=}N\text{-}SiMe_3$ afforded the U^V-imido complex **45**. Sequential reaction between **44** and $Me_3P{=}CH_2$ followed by $Me_3N^+\text{-}O^-$ afforded the corresponding U^V-oxo complex **47** (Scheme 2).

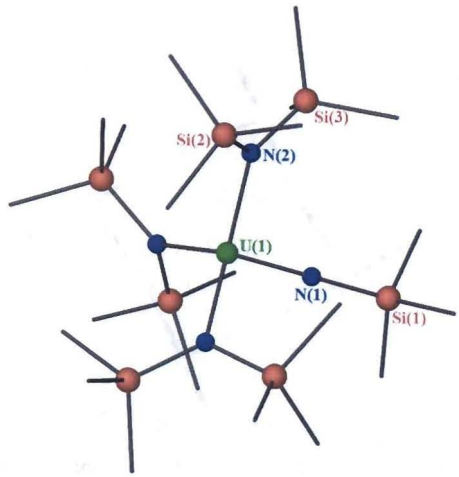

Figure 9 Ball-and-stick representation of $[N(SiMe_3)_2]_3U(=N\text{-}SiMe_3)$ (**43**).

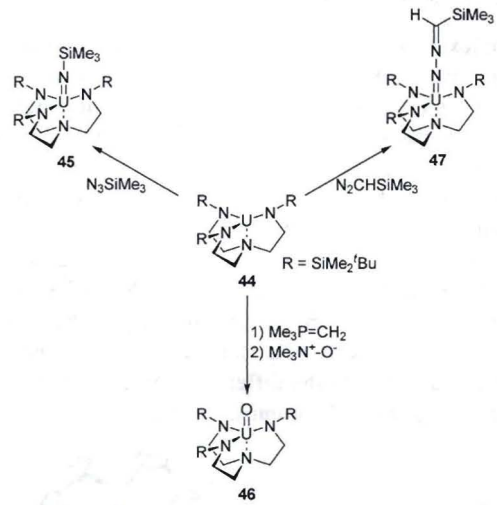

Scheme 2 Reaction manifold for the 2-electron oxidation of $(NN'_3)U$ (**44**).

In attempts to synthesize a uranium alkylidene complex, Scott and co-workers reacted **44** with 1 equiv. of trimethylsilyldiazomethane ($N{=}N{=}CHSiMe_3$). However, rather than forming an alkylidene complex through oxidative transfer of "$=CHSiMe_3$" to the uranium metal with loss of N_2, the U^V-imido complex **47** was formed. Efforts to promote N_2 loss from **47** were not successful.[54]

Meyer and co-workers have successfully utilized this 2-electron oxidation protocol for the synthesis of a variety of U^V complexes. The trivalent $[(^tBu\text{-}ArO)_3tacn]U$ complex (**48**) ($(^tBu\text{-}ArO)_3tacn$ = 1,4,7-tris(3,5-di-*tert*-butyl-2-hydroxybenzyl)-1,4,7-triazacyclononane) was readily oxidized with $N{=}N{=}N\text{-}SiMe_3$ to give the corresponding pentavalent $[(^tBu\text{-}ArO)_3tacn]U(=N\text{-}SiMe_3)$ complex **50** in 39% yield (eq. 10).[55] The molecular structure for one of the two independent molecules in the unit cell of **50** is presented

in Figure 10. Along with the short U=N_{imido} distance (U(1)-N(4) = 1.991(4) Å [1.985(5) Å]) and near linear U=N-Si angle (U(1)-N(4)-Si(1) = 168.9(3)° [178.5(3)°]), of particular interest is the decrease in the U-O distances (U-O_{ave} = 2.189 Å [2.203 Å]) in **50** relative to the U^{III} starting material (**48**, U-O_{ave} = 2.265 Å), indicative the change in ionic radius.[56] Similar chemistry was also observed for the more sterically saturated adamantyl derivative [(Ad-ArO)$_3$tacn]U (**49**) ((Ad-ArO)$_3$tacn = 1,4,7-tris(3,5-di-adamantyl-2-hydroxybenzyl)-1,4,7-triazacyclononane), which was oxidized to [(Ad-ArO)$_3$tacn]U(=N-SiMe$_3$) (**51**) in 65% yield.[57] Unlike **50**, the more sterically pressured **51** reacts with various small molecule π-acids such as carbon monoxide and isocyanides.

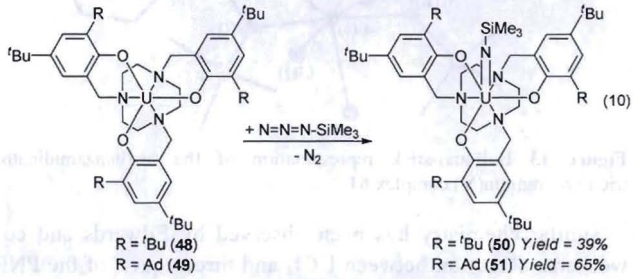

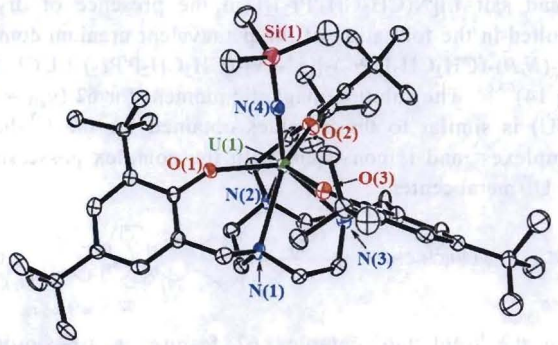

Figure 10 Molecular structure of [('Bu-ArO)$_3$tacn]U(=N-SiMe$_3$) (**50**).

In ongoing studies, the Meyer group has shown that the U^V-oxo complexes [('Bu-ArO)$_3$tacn]U(=O) (**54**) and [(Ad-ArO)$_3$tacn]U(=O) (**55**) can be formed by multiple-bond metathesis between the U^V-imido complexes [('Bu-ArO)$_3$tacn]U(=N-2,4,6-Me$_3$-C$_6$H$_2$) (**52**) and [(Ad-ArO)$_3$tacn]U(=N-2,4,6-Me$_3$-C$_6$H$_2$) (**53**), respectively, and CO_2 (eq. **11**).[58] Along with the generation of the thermodynamically stable mesityl isocyanate, the authors attribute the reactivity of these imido complexes to unfavorable steric congestion preventing optimal coordination of the bulky mesityl imido ligand – the U=N-C angle observed in the molecular structure of **52** is substantially less-linear (154.7(8)°) than that for the SiMe$_3$ variant **50** (U=N-Si = 173.7(3)°), thus resulting in a more energized molecular fragment (weaker U=N bond), which readily undergoes reaction. The [('Bu-ArO)$_3$tacn]U(=N-2,4,6-Me$_3$-C$_6$H$_2$) (**52**) and [(Ad-ArO)$_3$tacn]U(=N-2,4,6-Me$_3$-C$_6$H$_2$) (**53**) starting materials were formed by the reaction between the U^{III} starting complexes [('Bu-ArO)$_3$tacn]U (**48**) and [(Ad-ArO)$_3$tacn]U (**49**) and mesityl azide (94% and 96% yield, respectively).

Both [('Bu-ArO)$_3$tacn]U(=O) (**54**) and [(Ad-ArO)$_3$tacn]U(=O) (**55**) were structurally characterized, with the molecular structure of **55** shown in Figure **11**. The complexes are similar in constitution to their U^V-imido counterparts and have U=O_{oxo} distances of 1.848(8) Å (for **54**) and 1.848(4) Å (for **55**).

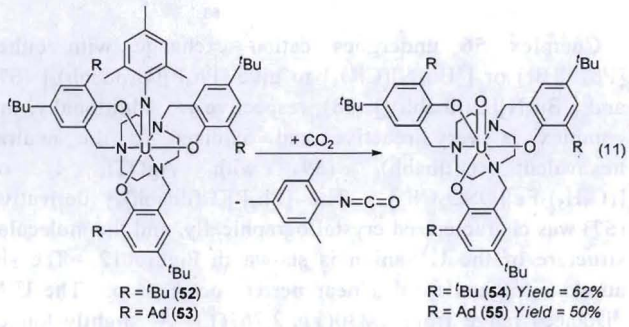

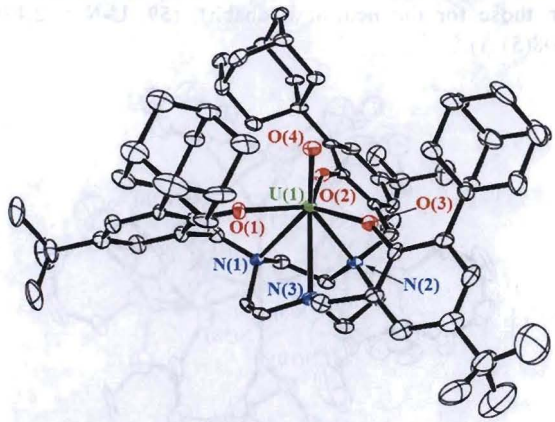

Figure 11 Molecular structure of [(Ad-ArO)$_3$tacn]U(=O) (**55**).

The variable temperature magnetic susceptibility of the [(ArO)$_3$tacn]U(=N-R) and [(ArO)$_3$tacn]U(=O) complexes were measured.[55,57,58] The imido complexes have effective magnetic moments of 2.34 (for **50**), 2.28 (for **51**), 2.35 (for **52**) and 2.40 (for **53**), while the oxo complexes have slightly lower values of 1.98 (for **54**) and 1.92 (for **55**). All values are in μ_B/U at 300 K. Although the imido complexes were EPR silent, the oxo complexes were EPR active, with **55** having $g_\perp$ = 1.14 and $g_\parallel$ = 2.15, consistent with a μ = ½ ground state. The authors suggest the U^V-imido and -oxo complexes possess different gound states.

The Cummins group has reported the synthesis of an anionic homoleptic amide U^V complex. Reaction between $UI_3(THF)_4$ (**33**) and 7 equiv. [Li(dbabh)(OEt$_2$)] (Hdbabh = 2,3:5,6-dibenzo-7-azabicyclo[2.2.1]hepta-2,5-diene) resulted in formation of the salt complex [Li(THF)$_n$][U(dbabh)$_6$] (**56**) in 89% yield (eq. 12).[59] This reaction is formally a 2-electron oxidation of the uranium metal, which presumably is accounted for by the additional equivalent of [Li(dbabh)(OEt$_2$)] utilized in the optimized reaction. In support of this, a stoichiometric (relative to U) amount of anthracene is produced in this reaction.

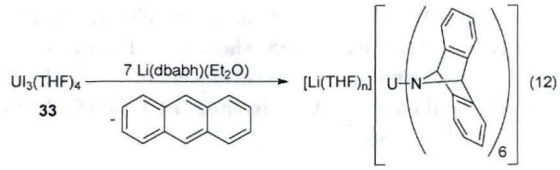

Complex **56** undergoes cation exchange with either $[Ph_4P][Br]$ or $[^nBu_4N][ClO_4]$ to give $[Ph_4P][U(dbabh)_6]$ (**57**) and $[^nBu_4N][U(dbabh)_6]$ (**58**), respectively. Additionally, the complex is very reactive and oxidized to the neutral hexavalent $U(dbabh)_6$ (**59**) with AgOTf, I_2 or $[(C_5H_5)_2Fe][OSO_2CF_3]$. The $[Ph_4P][U(dbabh)_6]$ derivative (**57**) was characterized crystallographically, and the molecular structure of the U^V anion is shown in Figure 12. The six amido nitrogens form a near perfect octahedron. The U-N distances range from 2.230(11)-2.267(13) Å, slightly longer than those for the neutral $U(dbabh)_6$ (**59**, U-N = 2.178(6)-2.208(5) Å).[59]

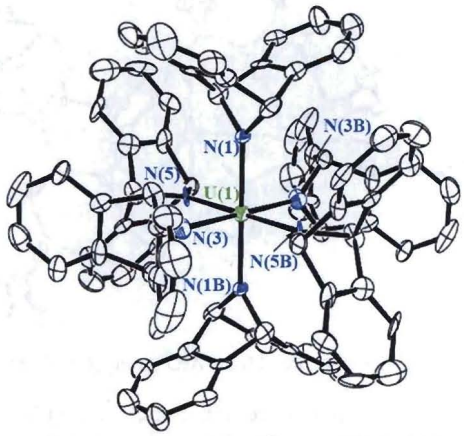

Figure 12 Molecular structure of the U^V anion $[U(dbabh)_6]^-$ in complex **57**.

Although EPR silent at room temperature, at 20 K the $[Li(THF)_n][U(dbabh)_6]$ complex **56** exhibits a single broad isotropic signal centered at |g| = 1.12 in its X-band EPR spectrum. The corresponding $[^nBu_4N][U(dbabh)_6]$ complex was characterized by magnetometry and had a μ_{eff} = 3.7 μ_B/U at 300 K.[59] These combined data are compatible with what is expected for a $5f^1$ U^V metal center in a high symmetry octahedral crystal field, perturbed by spin-orbit coupling.[2,60,61]

1-Electron Oxidation of Tetravalent Uranium

The 1-electron oxidation of tetravalent uranium has also proven to be a viable route into pentavalent uranium systems supported by amide and alkoxide ligands. Edelmann and co-workers reported the synthesis of a bis(benzamidinato)trichlorouranium(V) complex (**61**). Reaction of 2 equiv. of 4-Me-C_6H_4-C(=N-$SiMe_3$)N($SiMe_3$)$_2$ with UCl_4 (**60**) in the presence of dry O_2 yielded **61** cleanly and reproducibly, albeit in a low yield of 11% (eq. 13).[62] Formally a 1-electron oxidation of U^{IV}, the reaction was specific to oxidant, as similar reactions carried out with either $AgAsF_6$ or Cl_2 did not provide the desired U^V complex. The bis(benzamidinato)trichlorouranium(V) complex was characterized structurally and shown to have a seven-coordinate uranium ion featuring a distorted pentagonal-bipyramid geometry (Figure 13).

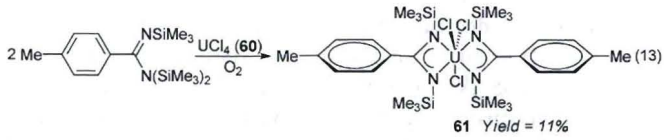

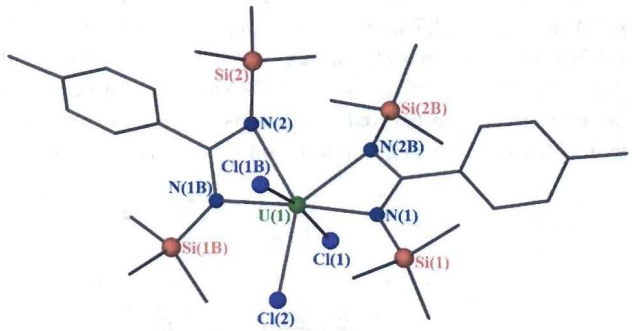

Figure 13 Ball-and-stick representation of the bis(benzamidinato) trichlorouranium(V) complex **61**.

Similar chemistry has been observed by Edwards and co-workers. Reaction between UCl_4 and three equiv. of the PNP ligand salt $Li[N(CH_2CH_2{}^iPr_2)_2]$ in the presence of dry O_2 resulted in the formation of the pentavalent uranium complex $[\kappa^2\text{-}(N,P)\text{-}(CH_2CH_2P^iPr_2)_2][\kappa^1\text{-}(N)\text{-}(CH_2CH_2P^iPr_2)_2]_2UCl_2$ (**62**) (eq 14)[63,64] The solution magnetic moment for **62** (μ_{eff} = 1.61 μ_B/U) is similar to those values obtained for the U^V-halide complexes[2] and is consistent with the complex possessing a $5f^1$ U^V metal center.

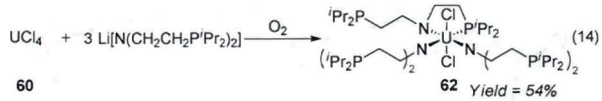

In the solid-state complex **62** features a six-coordinate uranium ion in a distorted octahedral geometry with two *trans* chlorides (Cl(1)-U(1)-Cl(2) = 172.83(4)°) and the three PNP ligands coordinated within the equatorial plane. One PNP ligand is bidentate with a κ^2-(*P*,*N*) coordination mode, while the other two PNP ligands are coordinated to the uranium in a monodentate κ^1-(*N*) fashion (Figure 14).

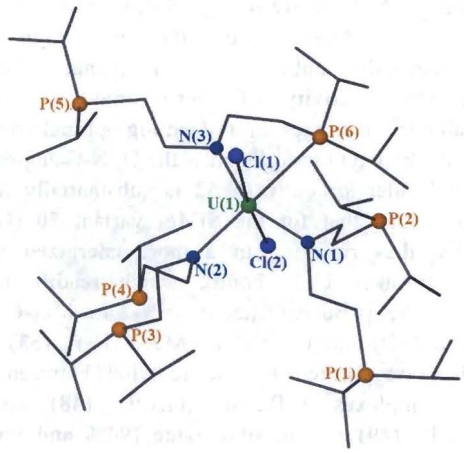

Figure 14 Ball-and-stick representation of $[\kappa^2\text{-}(N,P)\text{-}(CH_2CH_2P^iPr_2)_2][\kappa^1\text{-}(N)\text{-}(CH_2CH_2P^iPr_2)_2]_2UCl_2$ (**62**).

Salmon and coworker have reported the synthesis of a U^V complex supported by a calixarene ligand.[65] Reaction of H_4L^2 (H_4L^2 = *p-tert*-butyltetrahydroxy[3.1.3.1]metacyclophane) with UCl_4 in pyridine provided the complex [H-py][$UCl_2(L^2)$] (**63**) (eq. 15). The uranium metal is formally oxidized by 1-electron in this reaction.

$$H_4L^2 + UCl_4 \xrightarrow[\text{pyridine}]{} [\text{H-py}][UCl_2(L^2)] \quad (15)$$

60 **63**

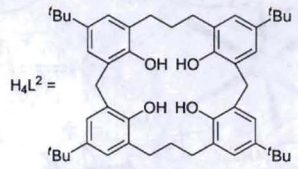

The molecular structure of complex **63** is provided in Figure 15. The uranium(V) ion is six-coordinate and possesses a slightly distorted octahedral geometry. The calixarene ligand adopts a cone conformation and sits on two of the bottom faces of the octahedron with the two chloride ligands being *cis* to each other (Cl(1)-U(1)-Cl(2) = 89.72(5)°).

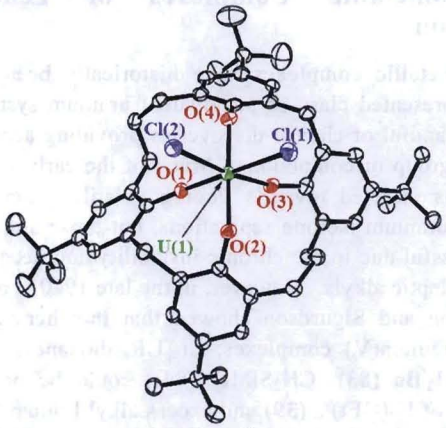

Figure 15 Molecular structure of the U^V anion in [H-py][$UCl_2(L^2)$] (**63**).

Ephritikhine and co-workers have also reported the synthesis of a bimetallic oxo-bridged U^V/U^V calixarene complex.[66] Reaction of calix[5]arene (H_5L^3) with an equivalent of UCl_4 in pyridine gave [H-py]$_2$[{U(L^3)}$_2$(μ_2-O)] (**64**) in 63% isolated yield (eq. 16). The $U^{IV} \rightarrow U^V$ oxidation was proposed to occur from the presence of adventitious water in the reaction mixture. Complex **64** was crystallographically characterized (Figure **16**). Using similar chemistry, bimetallic mixed-valent uranium(IV/V) calixarene complexes have also been prepared.[66,67]

$$H_5L^3 + UCl_4 \xrightarrow[\text{pyridine}]{} [\text{H-py}]_2[\{U(L^3)\}2(\mu_2\text{-O})] \quad (16)$$

60 **64** *Yield = 63%*

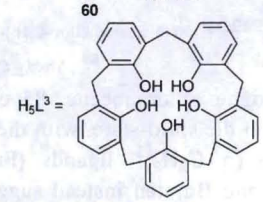

The tris(amido)amine ligand framework has also been successful in supporting a variety of pentavalent uranium amide and alkoxide complexes. Electrochemical studies on the [Li(THF)$_n$][(NN'$_3$)U(OR)(OR')] (NN'$_3$ = N($CH_2CH_2NSiMe_3$)$_3$; R = R' = Ph (**65**); R = Ph, R' = ^{t}Bu (**66**); R= R' = ^{t}Bu (**67**)) complexes showed quasi-reversible behavior with $E_{1/2}$ = 1.16 V (for **65**), -0.97 V (for **66**) and -1.04 V (for **67**) versus $[(C_5H_5)_2Fe]^{+/0}$. Inspired by these results, Scott and co-workers utilized $[(C_5Me_5)_2Fe][PF_6]$ as the oxidant to chemically prepare the neutral U^V complexes (NN'$_3$)U(OPh)$_2$ (**68**), (NN'$_3$)U(OPh)(O^{t}Bu) (**69**) and (NN'$_3$)U(O^{t}Bu)$_2$ (**70**) in 77%, 69% and 51% yields, respectively (eq. **17**).[68]

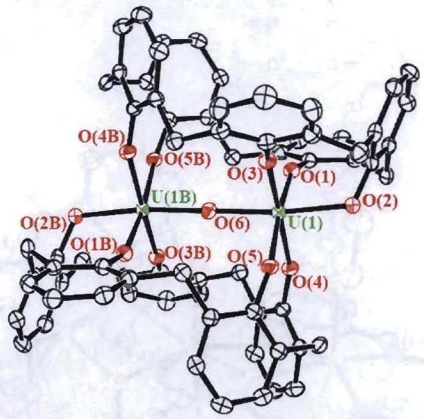

Figure 16 Molecular structure of the U^V/U^V anion in [H-py]$_2$[{U(L^3)}$_2$(μ_2-O)] (**64**).

$$[Li(THF)_n]\left[\text{Me}_3\text{Si}\text{-}\underset{\text{Me}_3\text{Si}}{\overset{\text{R}\quad\text{R}'}{\text{O}\quad\text{O}}}\text{U}\text{N}\text{-}\text{SiMe}_3\right] \xrightarrow[\text{- [Li(THF)}_n\text{][PF}_6\text{]}\ \text{- (C}_5\text{H}_5\text{)}_2\text{Fe}]{[(C_5H_5)_2Fe][PF_6]} \left[\text{Me}_3\text{Si}\text{-}\underset{\text{Me}_3\text{Si}}{\overset{\text{R}\quad\text{R}'}{\text{O}\quad\text{O}}}\text{U}\text{N}\text{-}\text{SiMe}_3\right] \quad (17)$$

R = R' = Ph (**65**)	R = R' = Ph (**68**)	*Yield = 77%*
R = Ph, R' = ^{t}Bu (**66**)	R = Ph, R' = ^{t}Bu (**69**)	*Yield = 69%*
R = R' = ^{t}Bu (**67**)	R = R' = ^{t}Bu (**70**)	*Yield = 51%*

Using silver(I) reagents, the Ephritikhine team demonstrated that 1-electron oxidation of trimetallic M-U^{IV}-M (M = Cu^{II}, Zn^{II}) complexes affords the corresponding U^V analogues.[69] Reaction of {CuL^4(pyridine)}$_2U^{IV}$ (**71**) (L^4 = *N,N'*-bis(3-hydroxysalicylidene)-1,3-propanediamine) with excess (3 equiv.) $AgNO_3$ resulted in the generation of the pentavalent uranium system [{CuL^4(pyridine)}$_2U^V$][NO_3] (**73**) in 28% isolated yield (eq. 18). Reaction of the zinc derivative {ZnL^4(pyridine)}$_2U^{IV}$ (**72**) to give [{ZnL^4(pyridine)}$_2U^V$][NO_3] (**74**) in 45% yield was also carried out, although in this case only 1 equiv. of the oxidant was required. Attempts to obtain analytically pure material of both **73** and **74** were not successful.

$$\{ML^4(\text{pyridine})\}_2U^{IV} \xrightarrow{1 \text{ or } 3\ AgNO_3} [\{ML^4(\text{pyridine})\}_2U^V][NO_3] \quad (18)$$

M = Cu (**71**)	M = Cu (**73**) *Yield = 28%*
M = Zn (**72**)	M = Zn (**74**) *Yield = 45%*

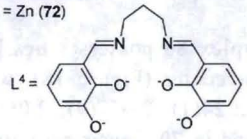

Switching to the *N,N'*-bis(3-hydroxysalicylidene)-1,4-butanediamine ligand (L^5) provided analytically pure samples of a M-U^V-M complex. Oxidation of {ZnL^5(pyridine)}$_2U^{IV}$

(**75**) with 1 equiv. $AgNO_3$ gave $[\{ZnL^5(pyridine)\}U^V\{ZnL^5(pyridine)_2\}][NO_3]$ (**76**) in 80% yield (eq 19). Complex **76** was structurally characterized (Figure 17). The two Zn atoms occupy the outer N_2O_2 cavities of the Schiff-base ligands, while the U^V atom is encapsulated by the eight oxygens atoms from the two Schiff-base ligands and features a dodecahedron geometry. The corresponding copper system was not prepared.[69]

$$\underset{\textbf{75}}{\{ZnL^5(pyridine)\}_2U^{IV}} \xrightarrow{AgNO_3} \underset{\textbf{76}\ \textit{Yield = 80\%}}{[\{ZnL^5(pyridine)\}U^V\{ZnL^5(pyridine)_2\}][NO_3]} \quad (19)$$

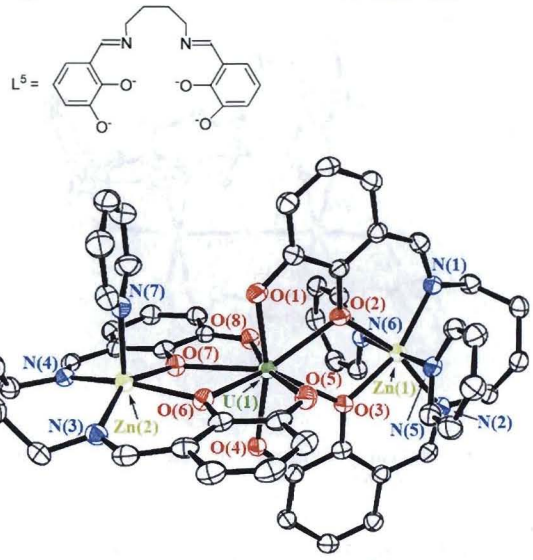

Figure 17 Molecular structure of the trimetallic $[\{ZnL^5(pyridine)\}U^V\{ZnL^5(pyridine)_2\}]^+$ cation in complex **76**.

In other work, Berthet and Ephritikhine reported the use of thallium(I) as an oxidant. Reaction of $Li[U(NEt_2)_5]$ (**77**) with $TlBPh_4$ afforded the homoleptic U^V-amide complex $U(NEt_2)_5$ (**78**) in 90% yield (eq. 20).[70]

$$\underset{\textbf{77}}{Li[U(NEt_2)_5]} \xrightarrow[-Tl^0,\ -LiBPh_4]{TlBPh_4} \underset{\textbf{78}\ \textit{Yield = 90\%}}{U(NEt_2)_5} \quad (20)$$

Recently, the Hayton group published a simple protocol for the synthesis of a homoleptic alkoxide uranium(V) complex.[71] Oxidation of $[Li(THF)]_2[U(O^tBu)_6]$ (**79**) with 0.5 equiv. I_2 results in formation of the complex $[Li(Et_2O)][U(O^tBu)_6]$ (**80**) in 25% yield (eq. 21). The analogous compound could be formed in much higher yield (98%) through the comproportionation of **79** and $U(O^tBu)_6$ (**81**) (eq. 22).

$$\underset{\textbf{79}}{[Li(THF)]_2[U(O^tBu)_6]} \xrightarrow[Et_2O,\ -LiI]{0.5\ I_2} \underset{\textbf{80}\ \textit{Yield = 25\%}}{[Li(Et_2O)][U(O^tBu)_6]} \quad (21)$$

$$\underset{\textbf{79}}{[Li(THF)]_2[U(O^tBu)_6]} + \underset{\textbf{81}}{U(O^tBu)_6} \xrightarrow{Et_2O} \underset{\textbf{80}\ \textit{Yield = 98\%}}{2\ [Li(Et_2O)][U(O^tBu)_6]} \quad (22)$$

In the solid-state, complex **80** possesses nearly octahedral geometry at the uranium center (Figure 18), with the U-O bond distances (U-O = 2.24(1), 2.059(9), 2.05(1) Å) being shorter than those observed in **79**, consistent with the smaller ionic radius of U^V.[56] The lithium ion is contained within the secondary coordination sphere and is ligated by two *tert*-butoxide ligands and one Et_2O molecule. The ^1H NMR spectrum of **80** in C_6D_6 exhibits a single, broad signal at δ 2.00 ppm, suggesting that in solution the Li^+ ion is rapidly exchanging among all possible binding locations.

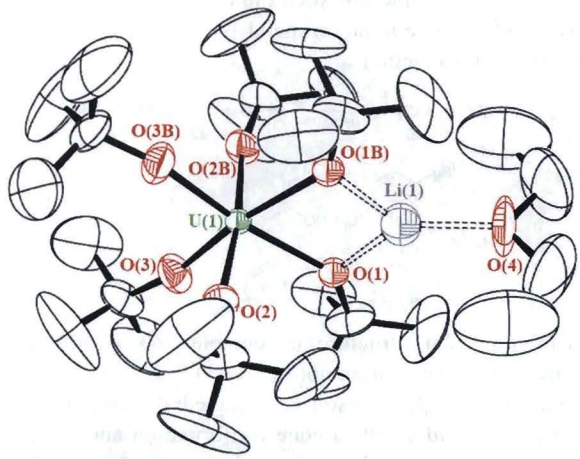

Figure 18 Molecular structure of $[Li(Et_2O)][U(O^tBu)_6]$ (**80**).

Organometallic Complexes of Pentavalent Uranium

Organometallic complexes have historically been the most underrepresented class of pentavalent uranium systems, with only a handful of chance discoveries providing access to this elusive group of compounds. Much of the early work in the field was directed towards finding volatile materials to be used in uranium isotope separations, but those attempts were unsuccessful due to the chronic instability and decomposition of homoleptic alkyls. However, in the late 1970's, a report by Wilkinson and Sigurdson showed that the thermally stable organouranium(V) complexes, $Li_3[UR_8(dioxane)_3]$ (R = Me (**82**), $CH_2{}^tBu$ (**83**), CH_2SiMe_3 (**84**)) could be prepared by reaction of $U_2(OEt)_{10}$ (**39**) and excess alkyl lithium (eq. 23).[72] Although not crystallographically characterized, the complexes could be isolated as green solids and analyzed by ^1H NMR spectroscopy.

$$\underset{\textbf{39}}{U_2(OEt)_{10}} + \text{excess LiR} \xrightarrow{dioxane} Li_3(dioxane)_3UR_8 \quad (23)$$

R = CH_3 (**82**)
R = $CH_2{}^tBu$ (**83**)
R = CH_2SiMe_3 (**84**)

In a landmark communication, Ephritikhine and co-workers reported the isolation of the first cycloheptatrienyl sandwich complex $[K(18\text{-crown-6})][U(\eta^7\text{-}C_7H_7)_2]$ (**85**) in 52% yield from the reaction between UCl_4, K^0 and excess cycloheptatriene (eq. 24).[73]

$$\underset{\textbf{60}}{UCl_4} + K^0 + \underset{\text{excess}}{\bigcirc} \xrightarrow{18\text{-crown-6}} \underset{\textbf{85}\ \textit{Yield = 52\%}}{[K(18\text{-crown-6})][U(\eta^7\text{-}C_7H_7)_2]} \quad (24)$$

Considered the f^1 analogue of uranocene, **85** exists as a discrete cation-anion pair in the solid-state, with the U^V anion sandwiched between two $(\eta^7\text{-}C_7H_7)^{3-}$ ligands (Figure 19). Theoretical studies by Li and Bursten instead suggested that complex **85** is best described as a U^{III} interacting with two $(\eta^7\text{-}C_7H_7)^{2-}$ ligands.[74] Subsequent EPR and angle-selected ENDOR spectroscopic studies confirmed the f^1 configuration of the compound with a ground state molecular orbital

comprised of both $5f_\pi$ (51%) and $5f_\sigma$ (39%). The principle values of the low temperature (15 K) EPR are $g_\perp$ = 2.365±0.005 and $g_\parallel$ = 1.244±0.005.[61]

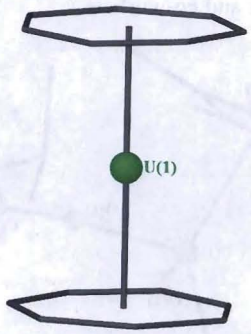

Figure 19 Ball-and-stick representation of the anion $[U(\eta^7\text{-}C_7H_7)_2]^-$ in complex (**85**).

In an attempt to prepare an organometallic uranium dioxo species, Burns, Clark and co-workers instead formed an unusual isopolyoxometalate cluster containing six U^V centers. Reaction of (1,2,4-^{t}Bu$_3$-C$_5$H$_2$)$_2$UCl$_2$ (**86**) with 2 equiv. of the reducing agent KC_8, followed by 2 equiv. of pyridine-*N*-oxide, afforded the multimetallic uranium complex (1,2,4-^{t}Bu$_3$-C$_5$H$_2$)$_4$U$_6$O$_{13}$(bpy)$_2$ (**87**) in 54% yield (eq. 25).[75]

$$\underset{\textbf{86}}{(1,2,4\text{-}{}^t\text{Bu}_3\text{-}C_5H_2)_2UCl_2} \xrightarrow[\text{2 pyridine-}N\text{-oxide}]{\text{2 KC}_8} \underset{\textbf{87}\ \textit{Yield = 54\%}}{(1,2,4\text{-}{}^t\text{Bu}_3\text{-}C_5H_2)_4U_6O_{13}(bpy)_2} \quad (25)$$

Complex **87** was crystallographically characterized, a representation of which is shown in Figure **20**. The complex consists of six uranium(V) atoms arranged in a *pseudo*-octahedral fashion linked by twelve μ_2-oxo bridging atoms. An interstitial μ_6-oxo atom sits in the center of the cluster, thus completing the $[U_6O_{13}]$ isopolyoxometalate core. Additionally, the four equatorial terminal uranium sites are bound to a (1,2,4-^{t}Bu$_3$-C$_5$H$_2$) ligand, while the axial uranium atoms are coordinated to a bidentate bipyridine (bpy) ligand. Although structurally similar to the Lindqvist class of polyoxometallate anions, there is no indication of electronic delocalization in the complex. A μ_{eff} = 1.8 μ_B per uranium was measured for the complex, which suggests that the six U^V centers behave as independent paramagnets.

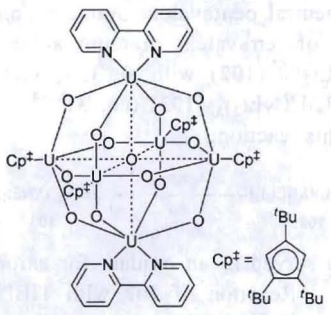

Figure 20 The (1,2,4-^{t}Bu$_3$-C$_5$H$_2$)$_4$U$_6$O$_{13}$(bpy)$_2$ (**87**) complex.

In their recent investigations of uranium linear metallocene complexes, Berthet, Ephritikhine and collaborators reported the isolation of the pentavalent uranium complex [^{n}Bu$_4$N]$_2$[(C$_5$Me$_5$)$_2$U(CN)$_5$] (**88**) which was proposed by the authors to have formed from oxidation of the parent U^{IV} complex by adventitious traces of air.[76] The molecular structure of the $[(C_5Me_5)_2U(CN)_5]^{2-}$ anion is shown in Figure 21.

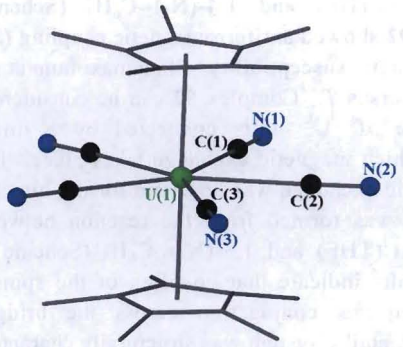

Figure 21 Ball-and-stick representation of the linear metallocene anion $[(C_5Me_5)_2U(CN)_5]^{2-}$ in complex (**88**)

The majority of U^V organometallic complexes have been prepared using more traditional strategies such as the 1- and 2-electron oxidation routes employed for the synthesis of uranium(V) amide and alkoxide systems discussed earlier. Details for each are provided in the following sections.

2-Electron Oxidation of Trivalent Uranium

The $U^{III} \rightarrow U^V$ conversion using 2-electron oxidizing agents has proven to be a viable route for accessing pentavalent organometallic uranium complexes. Andersen and co-workers reported the oxidation of (C$_5$H$_4$Me)$_3$U(THF) (**89**) with either the azide N=N=N-Ph or N=N=N-SiMe$_3$ gave the corresponding U^V-imido complexes (C$_5$H$_4$Me)$_3$U(=N-Ph) (**90**) or (C$_5$H$_4$Me)$_3$U(=N-SiMe$_3$) (**91**), respectively (eq. 26).[77] The reaction was noted to occur over a short (< 30 min) time frame with the evolution of N_2.

$$\underset{\textbf{89}}{(C_5H_4Me)_3U(THF)} \xrightarrow[-\ N_2]{+\ N{=}N{=}N\text{-}R} \underset{\substack{R = Ph\ (\textbf{90})\\ R = SiMe_3\ (\textbf{91})}}{(C_5H_4Me)_3U(=N\text{-}R)} \quad (26)$$

Complex **90** was characterized structurally (Figure 22). The most notable geometric parameters are the short U=N bond length (U(1)-N(1) = 2.019(6) Å) and essentially linear U=N-C angle (167.4(6)°). As with complex **43**, these data suggest that both lone pairs of the nitrogen atom are bonding to the uranium, creating a $U{=}N_{imido}$ linkage that is best viewed as a triple bond.

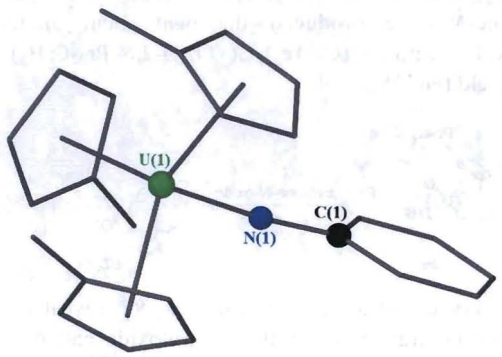

Figure 22 Ball-and-stick representation of (C$_5$H$_4$Me)$_3$U(=N-Ph) (**90**).

In an elegant study, Andersen and Edelstein went on to

show that analogous chemistry could be utilized to generate bimetallic U^V/U^V systems.[78] The bimetallic complex **92** was synthesized from the reaction between 2 equiv. $(C_5H_4Me)_3U(THF)$ and 1,4-$(N_3)_2$-C_6H_4 (Scheme 3, top). Complex **92** showed antiferromagnetic coupling ($J \sim -19$ cm^{-1}) in the magnetic susceptibility with a maximum at ~20 K in the plot of χ versus T. Complex **92** can be considered to be two monomeric $5f^1$ U^V units connected by a diimide ligand through which magnetic exchange takes place. Interestingly, no magnetic exchange was observed for the bimetallic system **93**, which was formed from the reaction between 2 equiv. $(C_5H_4Me)_3U(THF)$ and 1,3-$(N_3)_2$-C_6H_4 (Scheme 3, bottom). These results indicate that coupling of the spins on the U^V centers requires conjugation across the bridging ligand. Neither bimetallic system was structurally characterized.

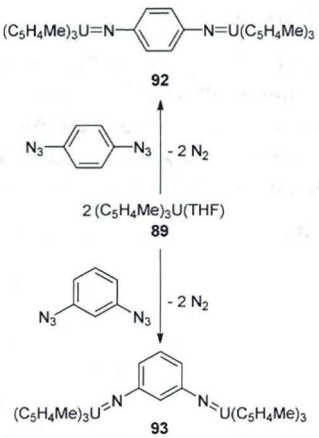

Scheme 3 Synthesis of the bimetallic U^V/U^V organometallic complexes **92** and **93**.

Lappert and Atwood also employed TMS-azide in the synthesis of a pentavalent uranium imido complex. Reaction of (1,3-^{t}Bu$_2$-C_5H_3)$_2$U(Cl)(THF) (**94**) with N=N=N-SiMe$_3$ resulted in formation of (1,3-^{t}Bu$_2$-C_5H_3)$_2$U(Cl)(=N-SiMe$_3$) (**95**) in 81% yield (eq. 27).[79] Characterization data for **95** was not provided.

$$\underset{\textbf{94}}{(1,3\text{-}^t\text{Bu}_2\text{-}C_5H_3)_2U(Cl)(THF)} \xrightarrow[-\ N_2]{+\ N{=}N{=}N\text{-}SiMe_3} \underset{\textbf{95}\ \textit{Yield = 81\%}}{(1,3\text{-}^t\text{Bu}_2\text{-}C_5H_3)_2U(Cl)(=N\text{-}SiMe_3)} \quad (27)$$

This oxidative atom transfer chemistry is not reserved for just azides. Arney and Burns demonstrated that reaction of $(C_5Me_5)_2U(O\text{-}2,6\text{-}^i Pr_2\text{-}C_6H_3)(THF)$ (**96**) with 1 equiv. pyridine-*N*-oxide produced the pentavalent uranium oxo aryloxide complex $(C_5Me_5)_2U(=O)(O\text{-}2,6\text{-}^i Pr_2\text{-}C_6H_3)$ (**97**) in 70% yield (eq. 28).[80]

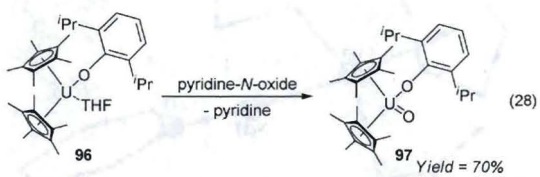

(28)

The crystal structure of complex **97** revealed a bent-metallocene framework with the aryloxide and oxo ligands contained within the metallocene wedge (Figure 23). The complex features a near linear U(1)-O(1)-C(21) angle of 169.7(5)° and a U=O_{oxo} bond distance of 1.859(6) Å, which is slightly longer than those seen for uranyl(V) complexes (U=O_{uranyl} = 1.810(4)-1.828(4) Å, *vide supra*) but similar to those oobserved in the uranium(V) oxo complexes **54** and **55** reported by Meyer and co-workers.

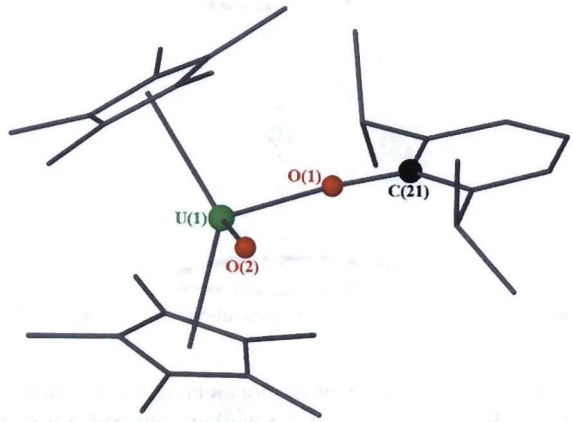

Figure 23 Ball-and-stick representation of $(C_5Me_5)_2U(=O)(O\text{-}2,6\text{-}^i Pr_2\text{-}C_6H_3)$ (**97**).

1-Electron Oxidations of Tetravalent Uranium

Pentavalent organouranium complexes have also been prepared using 1-electron oxidation of tetravalent uranium precursors. The Ephritikhine group has utilized silver(I) salts for the oxidation of a variety of organometallic uranium(IV) compounds.[81,82] Reaction of $(C_5Me_5)U(NMe_2)_3$ (**98**) with $AgBPh_4$ generated the first cationic uranium(V) complex $[(C_5Me_5)U(NMe_2)_3(THF)][BPh_4]$ (**99**) in 43% yield (eq. 29). Similarily, reaction between $(C_5Me_5)_2U(NEt_2)_2$ (**100**) with $AgBPh_4$ provided $[(C_5Me_5)_2U(NEt_2)_2][BPh_4]$ (**101**) in 74% yield (eq. 30). In both reactions a grey precipitate of metallic silver was noted.[83]

$$\underset{\textbf{98}}{(C_5Me_5)U(NMe_2)_3} \xrightarrow[-\ Ag^0]{AgBPh_4,\ THF} \underset{\textbf{99}\ \textit{Yield = 43\%}}{[(C_5Me_5)U(NMe_2)_3(THF)][BPh_4]} \quad (29)$$

$$\underset{\textbf{100}}{(C_5Me_5)_2U(NEt_2)_2} \xrightarrow[-\ Ag^0]{AgBPh_4,\ THF} \underset{\textbf{101}\ \textit{Yield = 74\%}}{[(C_5Me_5)_2U(NEt_2)_2][BPh_4]} \quad (30)$$

This oxidation procedure was also applicable to the synthesis of neutral pentavalent uranium complexes through the oxidation of tetravalent uranium anions. Reaction of $K[(C_8H_8)U(NEt_2)_3]$ (**102**) with $AgBPh_4$ yielded the neutral complex $(C_8H_8)U(NEt_2)_3$ (**103**) (eq. 31).[84] A yield was not provided for this reaction.

$$\underset{\textbf{102}}{K[(C_8H_8)U(NEt_2)_3]} \xrightarrow[-\ Ag^0\ -KBPh_4]{AgBPh_4} \underset{\textbf{103}}{(C_8H_8)U(NEt_2)_3} \quad (31)$$

$TlBPh_4$ also served as an oxidant for anionic uranium(IV) complexes.[70,84] Reaction of **102** with $TlBPh_4$ afforded the neutral complex $(C_8H_8)U(NEt_2)_3$ (**103**) in excellent yield (eq. 32). Both the lithium and sodium derivatives of the anionic starting complexes could also be oxidized. Interestingly, this Tl(I)-based protocol was specific to the electron-rich anions. Attempted oxidation of the neutral tetravalent complex $(C_8H_8)U(NEt_2)_2(THF)$ (**104**) with $TlBPh_4$ was unsuccessful.

However, utilization of the stronger oxidant $AgBPh_4$ did result in formation of the cationic U^V complex $[(C_8H_8)U(NEt_2)_2(THF)][BPh_4]$ (**105**) (Scheme 4).[84]

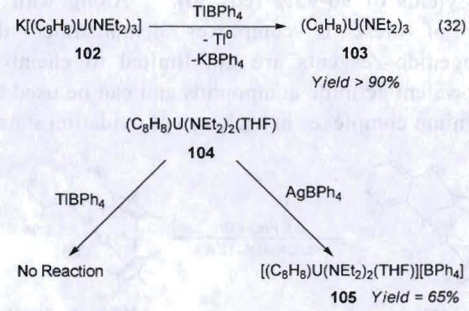

Scheme 4 Reaction of $(C_8H_8)U(NEt_2)_2(THF)$ (**104**) with the oxidizing agents $TlBPh_4$ and $AgBPh_4$.

Complexes **99**, **101** and **105** were all characterized by X-ray crystallography and shown to exist as discrete cation-anion pairs. The U^V cation in **99** (Figure 24) adopts a 5-coordinate *pseudo*-trigonal bipyramid geometry with the C_5Me_5 and THF ligands bound in a *trans* relationship and the three NMe_2 ligands residing in the equatorial plane. Both the $[(C_5Me_5)_2U(NMe_2)_2]^+$ and $[(C_8H_8)U(NEt_2)_2(THF)]^+$ cations feature a distorted tetrahedral geometry about the uranium metal center (Figures 25 and 26, respectively). Uranium L_{III}-edge X-ray absorption spectroscopy (EXAFS) was also used to analyze complex **105**;[85] the U-N (2.13 Å), U-C (2.66 Å) and U-O (2.41 Å) bond distances were consistent with those obtained from X-ray crystallography (U-N = 2.110(7), 2.121(7) Å; U-C = 2.66(1)-2.71(1) Å; U-O = 2.465(6) Å). EPR studies revealed that these $5f^1$ complexes all have $\mu = ½$ ground states and highly anisotropic |g| values ranging from 0.7-3.3, which are consistent with the lower symmetry of these complexes compared with the $[U(dbabh)_6]^-$ anion in complex **58**.[86]

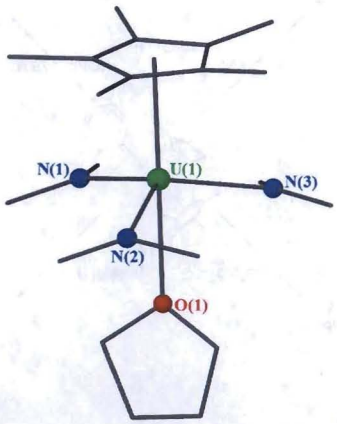

Figure 24 Ball-and-stick representation of the $[(C_5Me_5)U(NMe_2)_3(THF)]^+$ cation in complex **99**.

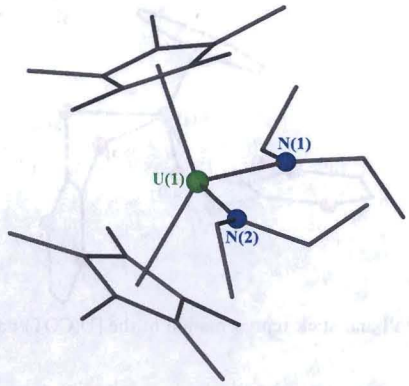

Figure 25 Ball-and-stick representation of the $[(C_5Me_5)_2U(NEt_2)_2]^+$ cation in complex **101**.

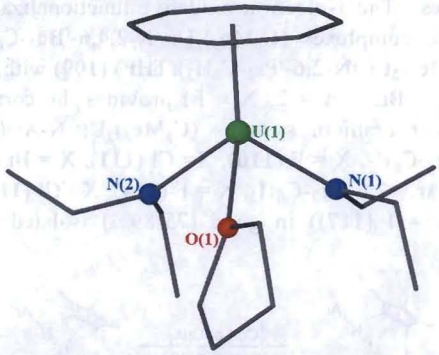

Figure 26 Ball-and-stick representation of the $[(C_8H_8)U(NEt_2)_2(THF)]^+$ cation in complex **105**.

Arliguie and collaborators also exploited the Ag(I) oxidation platform to access the first uranium(V) dithiolate complexes. Oxidation of the dianionic complex [Na(18-crown-6)]$_2$[U(COT)(dddt)$_2$] (**106**) (dddt = 5,6-dihydro-1,4-dithiin-2,3-dithiolate) with 1 equiv. $AgBPh_4$ afforded the corresponding pentavalent uranium complex [Na(18-crown-6)][U(COT)(dddt)$_2$] (**107**) quantitatively by ^1H NMR spectroscopy (eq. 33).[87]

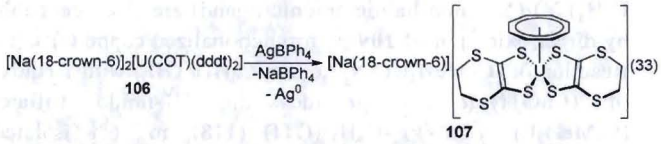

The uranium anion in **107** possesses a 5-coordinate, distorted square pyramidal geometry (Figure 27), with the dddt ligands arranged in an unusual *exo-endo* conformation. Electronic structure calculations revealed the *exo-endo* conformation is stabilized through an intramolecular U···(C=C) interaction involving the metal 5f orbitals and the C=C double bond of the *endo* dithiolene ligand.[88] No such interaction exists in the analogous uranium(IV) complex **106**, in which the diothiolene ligands exhibit an *exo-exo* conformation. This system has been studied in detail by DFT.

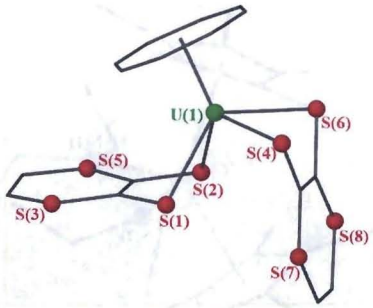

Figure 27 Ball-and-stick representation of the $[U(COT)(dddt)_2]^-$ anion in complex **107**.

Recently our group at Los Alamos discovered that copper(I) salts are ideal oxidants for the generation of U^V-imido complexes. The 1-electron oxidative functionalization of the U^{IV}-imido complexes $(C_5Me_5)_2U(=N\text{-}2,4,6\text{-}{}^tBu_3\text{-}C_6H_2)$ (**108**) and $(C_5Me_5)_2U(=N\text{-}2,6\text{-}{}^iPr_2\text{-}C_6H_3)(THF)$ (**109**) with CuX_n (n = 1, X = Cl, Br, I; n = 2, X = F) provides the corresponding pentavalent uranium systems $(C_5Me_5)_2U(=N\text{-}Ar)(X)$ (Ar = 2,4,6-${}^tBu_3$-C_6H_2, X = F (**110**), X= Cl (**111**), X = Br (**112**), X = I (**113**); Ar = 2,6-${}^iPr_2$-C_6H_3, X = F (**114**), X= Cl (**115**), X = Br (**116**), X = I (**117**)) in good (75-89%) isolated yields (eq 34).[89,90]

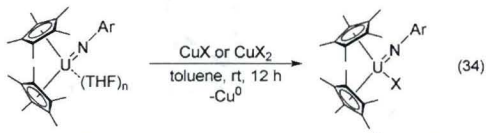

(34)

108: Ar = 2,4,6-${}^tBu_3$-C_6H_2, n = 0

Ar = 2,4,6-${}^tBu_3$-C_6H_2
110: X = F *Yield = 81%*
111: X = Cl *Yield = 75%*
112: X = Br *Yield = 77%*
113: X = I *Yield = 78%*

109: Ar = 2,6-${}^iPr_2$-C_6H_3, n = 1

Ar = 2,6-${}^iPr_2$-C_6H_3
114: X = F *Yield = 89%*
115: X = Cl *Yield = 80%*
116: X = Br *Yield = 88%*
117: X = I *Yield = 81%*

Non-halide uranium(V) derivatives $(C_5Me_5)_2U(=N\text{-}2,6\text{-}{}^iPr_2\text{-}C_6H_3)(Y)$ (Y = non-halide anionic ligand) are also accessible by direct oxidation of **109** with functionalized copper(I) salts. Reaction of $(C_5Me_5)_2U(=N\text{-}2,6\text{-}{}^iPr_2\text{-}C_6H_3)(THF)$ with 1 equiv. of $(CuOTf)_2$·toluene provides the U^V-imido triflate, $(C_5Me_5)_2U(=N\text{-}2,6\text{-}{}^iPr_2\text{-}C_6H_3)(OTf)$ (**118**), in 76% isolated yield (eq. 35).[89,91] Although elevated temperatures (75 °C) were required, similar chemistry utilizing CuSPh (5 equiv.) affords $(C_5Me_5)_2U(=N\text{-}2,6\text{-}{}^iPr_2\text{-}C_6H_3)(SPh)$ (**119**) in 90% yield (eq. 35).[89,91] Direct formation of a U-C bond is also possible using this oxidative pathway. Reaction of **109** and Cu-C≡C-Ph at 75 °C produced the U^V-acetylide complex $(C_5Me_5)_2U(=N\text{-}2,6\text{-}{}^iPr_2\text{-}C_6H_3)(C{\equiv}C\text{-}Ph)$ (**120**) in 58% yield (eq. 35).[92]

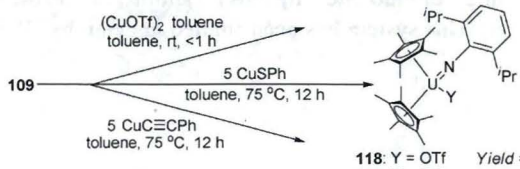

(35)

118: Y = OTf *Yield = 76%*
119: Y = SPh *Yield = 90%*
120: Y = C≡CPh *Yield = 58%*

This oxidative functionalization chemistry is not limited to Cu(I)-based oxidants. Reaction of **109** with 0.5 equiv. PhE-EPh yielded the chalcogen complexes $(C_5Me_5)_2U(=N\text{-}2,6\text{-}{}^iPr_2\text{-}C_6H_3)(EPh)$ (E = S (**119**), Se (**121**), Te (**122**)) in excellent isolated yields of 90-95% (eq. 36).[93] Along with **107**, the stability of these U^V-complexes demonstrated that soft dichalcogenide reagents are not limited to chemistry with soft/low-valent actinide compounds and can be used to access hard uranium complexes in high-valent oxidation states.

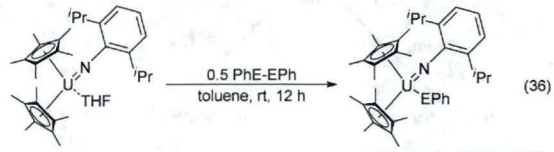

(36)

109

119: E = S *Yield = 94%*
121: E = Se *Yield = 90%*
122: E = Te *Yield = 95%*

A variety of other substituted U^V-imido complexes were available utilizing standard inorganic synthetic routes. Salt metathesis between $(C_5Me_5)_2U(=N\text{-}2,6\text{-}{}^iPr_2\text{-}C_6H_3)(I)$ (**117**) and either $KNPh_2$ or KOPh resulted in the complexes $(C_5Me_5)_2U(=N\text{-}2,6\text{-}{}^iPr_2\text{-}C_6H_3)(NPh_2)$ (**123**) and $(C_5Me_5)_2U(=N\text{-}2,6\text{-}{}^iPr_2\text{-}C_6H_3)(OPh)$ (**124**), respectively (Scheme 5). Complex **117** also served as a useful platform for the synthesis of both U^V-imido alkyl and aryl compounds. Reaction between **117** and either Me_2Mg or $Ph_2Mg(THF)_2$ afforded the alkyl ($(C_5Me_5)_2U(=N\text{-}2,6\text{-}{}^iPr_2\text{-}C_6H_3)(Me)$ (**125**)) and aryl ($(C_5Me_5)_2U(=N\text{-}2,6\text{-}{}^iPr_2\text{-}C_6H_3)(Ph)$ (**126**)) complexes, respectively (Scheme 5). Paired with **120**, the isolation of **125** and **126** shows that U^V can support the full range of carbon anions (sp, sp^2 and sp^3).[91] Importantly, these provided the first discrete examples of pentavalent uranium complexes with anionic carbon moieties other than the carbocyclic (C_5R_5, C_7H_7, C_8H_8) ligands.

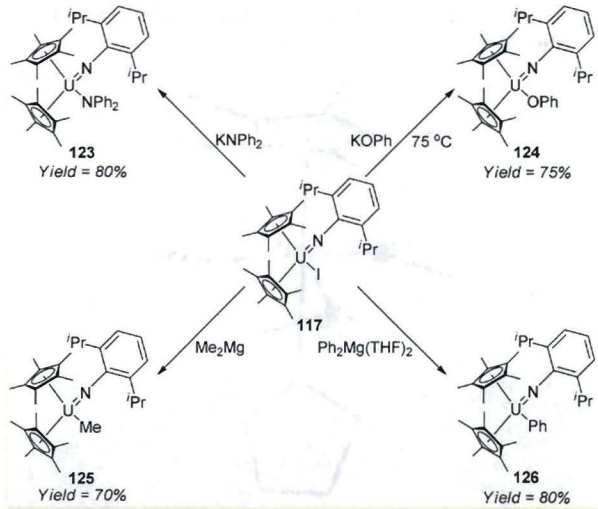

Scheme 5 Salt metathesis route to U^V-imido complexes **123-126**.

The U^V-imido ketimide complex $(C_5Me_5)_2U(=N\text{-}2,6\text{-}{}^iPr_2\text{-}C_6H_3)(N{=}CPh_2)$ (**127**) could be prepared by two different pathways. Complex **127** was formed in 86% isolated yield through the protonolysis reaction between $(C_5Me_5)_2U(=N\text{-}2,6\text{-}{}^iPr_2\text{-}C_6H_3)(Me)$ (**125**) and excess benzophenone imine at 75 °C. Alternatively, insertion of benzonitrile into the U-C_{aryl} bond of $(C_5Me_5)_2U(=N\text{-}2,6\text{-}{}^iPr_2\text{-}C_6H_3)(Ph)$ (**126**) gave **127** in

91% yield (eq. 37).[91]

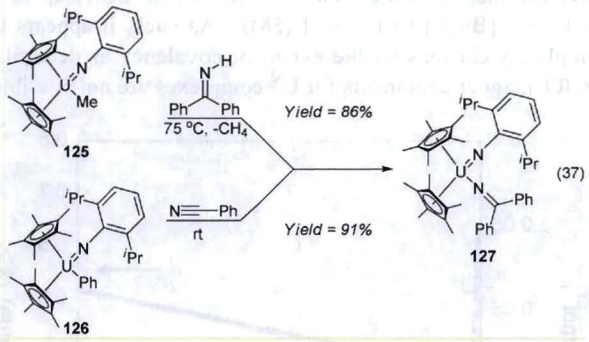

The development of this body of uranium(V) chemistry is important from a number of perspectives: (1) It not only complements the other routes to U^V organometallic complexes (*vide supra*), but shows that a wide array of classic reaction pathways – direct oxidation of U^{IV}, salt metathesis, protonolysis, and insertion – can be used to access functionalized uranium(V) systems; (2) That a wide range of electronically diverse substituents can be supported within the wedge of the $(C_5Me_5)_2U(=N\text{-}Ar)$ framework refutes prior assertions that pentavalent organouranium complexes are inherently unstable; and (3) For the first time since the archetypical halide and oxo halide compounds, a library of structurally related complexes could be prepared. This enabled the first systematic studies to interrogate the "rare" uranium(V) oxidation state using a combination of single-crystal X-ray diffraction, ^1H NMR spectroscopy, elemental analysis, mass spectrometry, cyclic voltammetry, UV-visible-NIR absorption spectroscopy, uranium L_{III}-EXAFS, density functional theory, and variable-temperature magnetic susceptibility.

The majority of these U^V-imido complexes were characterized by single-crystal X-ray diffraction studies. The molecular structures for both the ^{t}Bu and ^{i}Pr U^V-imido complexes feature a bent-metallocene framework with the imido and auxiliary ligands contained within the metallocene wedge, similar in constitution to the related U^V-oxo alkoxide complex $(C_5Me_5)_2U(=O)(O\text{-}2,6\text{-}^iPr_2\text{-}C_6H_3)$ (**97**).[80] Representative structures of $(C_5Me_5)_2U(=N\text{-}2,4,6\text{-}^tBu_3\text{-}C_6H_2)(I)$ (**113**) and $(C_5Me_5)_2U(=N\text{-}2,6\text{-}^iPr_2\text{-}C_6H_3)(I)$ (**117**) are shown in Figures 28 and 29, respectively, and selected geometric parameters for all of the crystallographically characterized complexes are provided in Table 2.

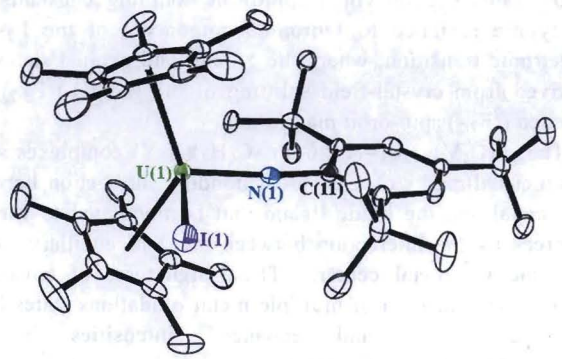

Figure 28 Molecular structure of $(C_5Me_5)_2U(=N\text{-}2,4,6\text{-}^tBu_3\text{-}C_6H_2)(I)$ (**113**).

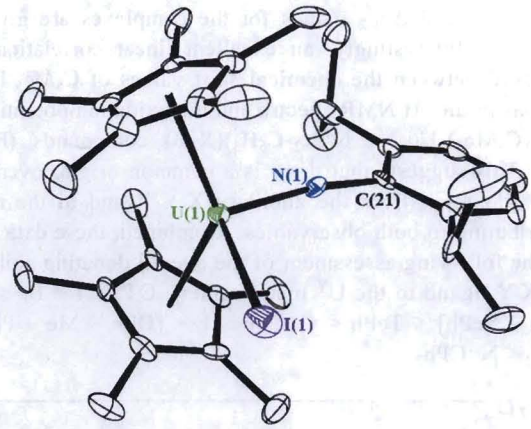

Figure 29 Molecular structure of $(C_5Me_5)_2U(=N\text{-}2,6\text{-}^iPr_2\text{-}C_6H_3)(I)$ (**117**).

In all cases, the $U{=}N_{imido}$ linkage is best viewed as having triple bond character, as indicated by short U=N distances (1.9575(5)-2.012(4) Å) and linear U-N-C_{Ar} angles (168.3(5)-174.6(4)°), which compare well with the U^V-imido parameters observed for other structurally characterized systems (*vide supra*). Bonding analysis using DFT on the model complexes $(C_5Me_5)_2U(=N\text{-}Ph)(F)$ (**128**) and $(C_5Me_5)_2U(=N\text{-}Ph)(I)$ (**129**) supports these findings and describes the multiple bonding between the uranium metal center and imido nitrogen as consisting of one σ- and two π-interactions with variable participation of 5f and 6d orbitals from the uranium center.[90] The X/Y ligand did not significantly influence the imido parameters. However, as expected on the basis of the ionic radius of the X/Y atom[56] the U-X/Y bond length decreases down the series, with U-F < U-N_{sp^2} < U-N_{sp^3} < U-Cl < U-S < U-Br < U-Se < U-I < U-Te.

Additional structural information was obtained for $(C_5Me_5)_2U(=N\text{-}2,4,6\text{-}^tBu_3\text{-}C_6H_2)(Cl)$ (**111**) by analyzing the uranium L_{III}-edge X-ray absorption spectrum. A U-N distance of 1.97(1) Å was measured, which is consistent with the formulation of a $U{=}N_{imido}$ bond and is similar to the structural data observed for the other structurally characterized U^V-imido complexes (Table 2). A U-Cl distance of 2.60(2) Å was also determined for **111**, which is similar to the U-Cl distance (2.621(2) Å) in complex **115**.

All of these systems exhibit two chemically reversible one-electron redox transformations; an oxidation wave attributable to the U^{VI}/U^V process and a reduction wave corresponding to the U^V/U^{IV} redox couple (Table 3). The redox activity in these compounds is dominated by the $(C_5Me_5)_2U{=}N\text{-}Ar$ core, as signified by a constant spacing (~1.50 V) between the reduction and oxidation processes. The variability in the half-wave potentials for these metal-based redox transformations across this series reflects the role of the ancillary ligand in perturbing the redox energetics in these systems. The overall effect across the series is quite dramatic for a seemingly small structural perturbation to the otherwise constant U^V-imido core – if one considers the potential of the U^{VI}/U^V oxidation wave, the process shifts by ~0.7 V on going from the triflate complex (**118**) to the ketimide complex (**127**).

The ^1H NMR spectra for these systems exhibit a broad signal at ~3-6 ppm corresponding to the $C_5\mathit{Me}_5$ ligand protons and inequivalent *ortho* ^{t}Bu or ^{i}Pr groups. The $C_5\mathit{Me}_5$

resonances and $\Delta\nu_{1/2}$ values for the complexes are given in Table 3. Interestingly, an excellent linear correlation was observed between the chemical shift values of C_5Me_5 ligand protons in the ^{1}H NMR spectra and the oxidation potentials of the $(C_5Me_5)_2U(=N\text{-}2,6\text{-}^iPr_2\text{-}C_6H_3)(X/Y)$ compounds (Figure 30). This suggests that there is a common origin, overall σ- and π-donation from the ancillary X/Y ligand to the metal, contributing to both observables. Combined, these data allow for the following assessment of the overall donating ability of the X/Y ligand to the U^V metal center: OTf < I < Br < Cl < [SPh ~ SePh] < TePh < C≡CPh < F < [OPh ~ Me ~ Ph] << NPh_2 < $N{=}CPh_2$.

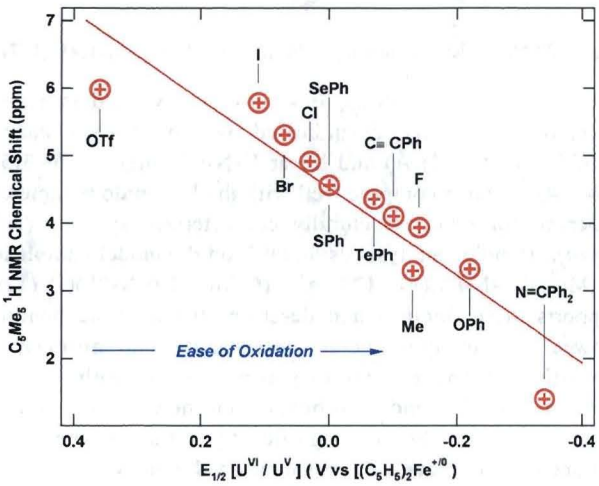

Figure 30 Linear correlation between ^{1}H NMR chemical shift of the C_5Me_5 protons and oxidation potential for $(C_5Me_5)_2U(=N\text{-}2,6\text{-}^iPr_2\text{-}C_6H_3)(X/Y)$ ($R^2 = 0.92$).

The magnetic response of the complexes is consistent with a U^V ion. As with the $\{[U^VO_2(py)_5][KI_2(py)_2]\}_\infty$ (**31**) system outlined earlier, a plot of the χT product versus T shows two distinct temperature regimes: a linear high temperature regime from ~40-300 K with a large slope and a low temperature regime <40 K where the χT products decrease precipitously. Figure 31 shows a representative plot of χT versus T and χ versus T for a U^V ion.

Effective magnetic moments in the range of 2.03-2.65 μ_B/U were observed for these complexes with no significant differences in μ_{eff} values or temperature dependencies based on X/Y (Table 3). At this point, uranium(V) magnetism deserves some special attention. Older reports of U^V paramagnetism have asserted the generally low magnetic moments for U^V complexes (compared to the *L-S* predicted value of 2.54 μ_B) arise from covalent character of the metal-ligand interaction that presumably results from siphoning of spin density from the metal to the ligand with an associated reduction in the orbital magnetism.[45] This would result in large differences in the RT magnetic moment for the complexes dependent on geometry and the extent of metal-ligand overlap. However, from our studies and those discussed throughout this article, one sees that no correlation exists between complexes that would be expected to show such a reduction due to large covalent metal-ligand interactions and those whose interactions are more ionic in nature. Indeed, reported μ_{eff} values for U^V systems are all over the map, ranging from 1.42 μ_B/U (for UCl_5) up to 3.7 μ_B/U (for $[Bu_4N][U(dbabh)_6]$ (**58**)). As such, it appears that simple conclusions on the extent of covalency as determined by RT magnetic moments for U^V complexes are not possible.

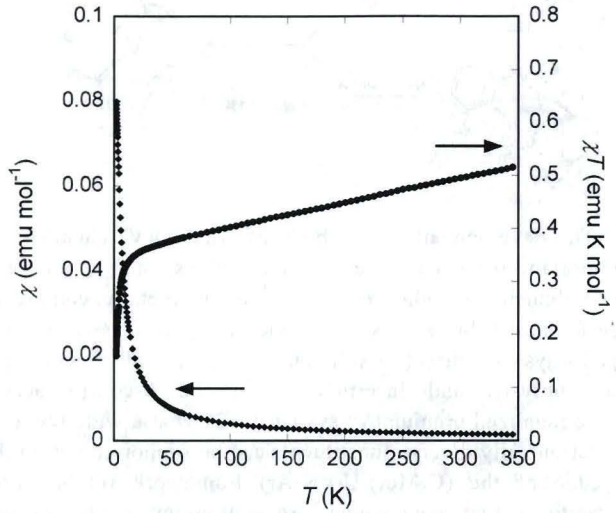

Figure 31 Representative temperature dependent magnetic susceptibility data for the $5f^1$ U^V ion in the U^V-imido complexes. The specific data in this figure corresponds to the $(C_5Me_5)_2U(=N\text{-}2,6\text{-}^iPr_2\text{-}C_6H_3)(I)$ complex **117**.

The electronic spectra for the C_s symmetric $(C_5Me_5)_2U(=N\text{-}Ar)(X/Y)$ complexes are comprised of $\pi\rightarrow\pi^*$ and $\pi\rightarrow nb_{5f}$ transitions involving electrons in the metal-imido bond, and metal-centered f-f bands illustrative of spin-orbit and crystal-field influences on the $5f^1$ valence electron configuration. Two distinct sets of bands have been attributed to transitions derived from this $5f^1$ configuration. A representative UV-vis-NIR absorption spectrum for a $(C_5Me_5)_2U(=N\text{-}2,6\text{-}^iPr_2\text{-}C_6H_3)(X/Y)$ complexes is presented in Figure 32. The UV-visible region displays broad, relatively intense bands ascribed principally to $\pi_{U=N}\rightarrow nb_{5f}$ transitions similar to those ligand-to-metal transitions seen in early transition-metal imido complexes.[94] Additional narrow, relatively weak bands in the near-IR region arise from intraconfiguration (f-f) transitions associated with the $5f^1$ valence electronic structure. Although much more intense, these f-f bands are comparable in energy and structure to those reported for U^V halides in much higher symmetry (O_h) environments, which suggests comparable (~2000 cm^{-1}) spin-orbit coupling constants.[95-97] They are assigned to vibronic components of the $\Gamma_7\rightarrow\Gamma_7$, electronic transition, where the ground and excited states are derived from crystal-field splitting of the ground ($^2F_{5/2}$) and excited ($^2F_{7/2}$) spin-orbit manifolds.

These $(C_5Me_5)_2U(=N\text{-}2,6\text{-}^iPr_2\text{-}C_6H_3)(X/Y)$ complexes show distinct hallmarks of a covalent bonding interaction between the metal and the imide ligand that is modulated to varying degrees by the interaction between the X/Y ancillary ligand and the U^V metal center. These signatures of covalency include stabilization of multiple metal oxidations states [U^{VI}, U^V, and U^{IV}] and enhanced intensities in the intraconfiguration (f-f) transitions.

Table 2 Selected geometric parameters for the structurally characterized $(C_5Me_5)_2U(=N\text{-}Ar)(X/Y)$ complexes.

	Ar	X/Y	Imido Parameters			X/Y Ligand Parameters		N_{imido}-U-X/Y
			U=N (Å)	N-C (Å)	U=N-C (°)			
110	2,4,6-^{t}Bu$_3$-C$_6$H$_2$	F	1.965(8)	1.415(11)	171.0(7)	**U-F (Å)** 2.122(5)		**N-U-F (°)** 97.0(3)
112	2,4,6-^{t}Bu$_3$-C$_6$H$_2$	Br	1.958(6)	1.424(9)	169.8(5)	U-Br (Å) 2.7744(10)		**N-U-Br (°)** 96.11(18)
113	2,4,6-^{t}Bu$_3$-C$_6$H$_2$	I	1.975(6)	1.418(8)	169.7(5)	U-I (Å) 3.0116(6)		**N-U-I (°)** 97.20(16)
115	2,6-^{i}Pr$_2$-C$_6$H$_3$	Cl	1.963(4)	1.404(7)	169.6(4)	**U-Cl (Å)** 2.6209(15)		**N-U-Cl (°)** 105.79(13)
116	2,6-^{i}Pr$_2$-C$_6$H$_3$	Br	1.969(7)	1.40(2)	172.2(9)	**U-Br (Å)** 2.789(3)		**N-U-Br (°)** 105.3(2)
117	2,6-^{i}Pr$_2$-C$_6$H$_3$	I	1.974(7)	1.406(10)	170.7(6)	**U-I (Å)** 3.0385(7)		**N-U-I (°)** 106.6(2)
118	2,6-^{i}Pr$_2$-C$_6$H$_3$	OTf	1.9575(5)	1.416(8)	168.3(5)	**U-O (Å)** 2.378(4)	**U-O-S (°)** 160.4(3)	**N-U-O (°)** 109.16(19)
119	2,6-^{i}Pr$_2$-C$_6$H$_3$	SPh	1.976(4)	1.398(6)	171.6(3)	**U-S (Å)** 2.7230(13)	**U-S-C (°)** 131.08(17)	**N-U-S (°)** 103.35(12)
121	2,6-^{i}Pr$_2$-C$_6$H$_3$	SePh	1.984(4)	1.403(6)	171.4(3)	**U-Se (Å)** 2.8639(6)	**U-Se-C (°)** 126.41(15)	**N-U-Se (°)** 102.17(11)
122	2,6-^{i}Pr$_2$-C$_6$H$_3$	TePh	1.960(6)	1.407(10)	170.6(6)	**U-Te (Å)** 3.0845(9)	**U-Te-C (°)** 121.5(2)	**N-U-Te (°)** 107.53(18)
123	2,6-^{i}Pr$_2$-C$_6$H$_3$	NPh$_2$	1.984(4)	1.399(6)	174.0(3)	**U-N (Å)** 2.322(4)		**N-U-N (°)** 93.73(15)
127	2,6-^{i}Pr$_2$-C$_6$H$_3$	N=CPh$_2$	2.012(4)	1.391(7)	174.6(4)	**U-N (Å)** 2.199(4)	**U-N-C (°)** 177.8(4)	**N-U-N (°)** 111.99(17)

Table 3 Selected characterization data for the $(C_5Me_5)_2U(=N\text{-}Ar)(X/Y)$ complexes.

	Ar	X/Y	^{1}H NMR Data for C_5Me_5		Electrochemical Data[a]		μ_{eff} (μ_B/U)
			δ (ppm)	$\Delta\nu_{1/2}$ (Hz)	$E_{1/2}$ (U^{VI}/U^{V}) (V)	$E_{1/2}$ (U^{V}/U^{IV}) (V)	
110	2,4,6-^{t}Bu$_3$-C$_6$H$_2$	F	4.10	----[b]	-0.19	-1.78	2.46
111	2,4,6-^{t}Bu$_3$-C$_6$H$_2$	Cl	5.15	----[b]	0.04	-1.50	2.51
112	2,4,6-^{t}Bu$_3$-C$_6$H$_2$	Br	----[b]	----[b]	0.04	-1.43	2.30
113	2,4,6-^{t}Bu$_3$-C$_6$H$_2$	I	----[b]	----[b]	0.04	-1.25	2.53
114	2,6-^{i}Pr$_2$-C$_6$H$_3$	F	3.94	109	-0.14	-1.81	2.22
115	2,6-^{i}Pr$_2$-C$_6$H$_3$	Cl	4.92	84	0.03	-1.52	2.42
116	2,6-^{i}Pr$_2$-C$_6$H$_3$	Br	5.31	72	0.07	-1.44	2.42
117	2,6-^{i}Pr$_2$-C$_6$H$_3$	I	5.78	125	0.11	-1.37	2.34
118	2,6-^{i}Pr$_2$-C$_6$H$_3$	OTf	5.98	104	0.36	-1.21	2.65
119	2,6-^{i}Pr$_2$-C$_6$H$_3$	SPh	4.57	83	0.00	-1.43	2.48
120	2,6-^{i}Pr$_2$-C$_6$H$_3$	C≡C-Ph	4.11	80	-0.10	-1.64	2.22
121	2,6-^{i}Pr$_2$-C$_6$H$_3$	SePh	4.57	147	0.00	-1.43	----[c]
122	2,6-^{i}Pr$_2$-C$_6$H$_3$	TePh	4.36	172	-0.07	-1.44	----[c]
123	2,6-^{i}Pr$_2$-C$_6$H$_3$	NPh$_2$	----[d]	----[d]	-0.30	-1.65	2.27
124	2,6-^{i}Pr$_2$-C$_6$H$_3$	OPh	3.33	71	-0.22	-1.75	2.38
125	2,6-^{i}Pr$_2$-C$_6$H$_3$	Me	3.30	63	-0.13	-1.71	----[c]
126	2,6-^{i}Pr$_2$-C$_6$H$_3$	Ph	3.00	117	----[e]	----[e]	----[c]
127	2,6-^{i}Pr$_2$-C$_6$H$_3$	N=CPh$_2$	1.41	52	-0.34	-1.84	2.03

[a] All versus $[(C_5H_5)_2Fe]^{+/0}$. [b] The C_5Me_5 resonance occurred in the same position one of the ^{t}Bu resonances and an accurate position was not possible. [c] Not measured. [d] No resonances assignable to the C_5Me_5 protons were observed in the ^{1}H NMR spectrum of **123** over the temperature range 0-100 °C. [e] Rapid decomposition of complex **126** in the supporting electrolyte solution prohibited data collection.

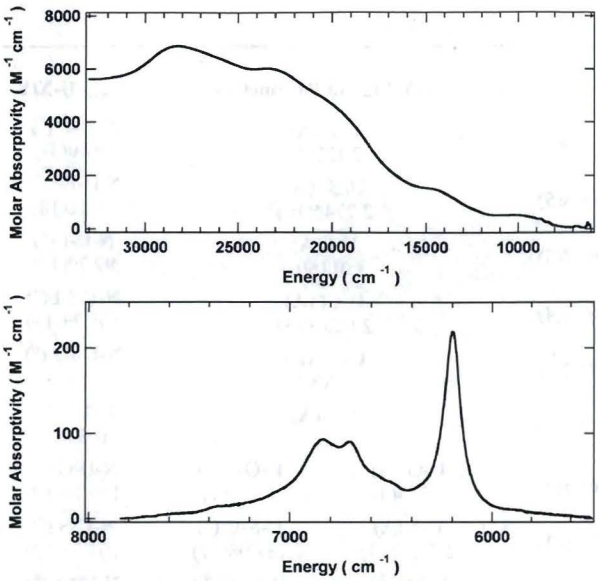

Figure 32 Representative electronic absorption spectral data for the ^{i}Pr-U^{V}-imido complexes. The specific data in this figure corresponds to the $(C_5Me_5)_2U(=N\text{-}2,6\text{-}^{i}Pr_2\text{-}C_6H_3)$(I) complex **117**.

Conclusions and Outlook

The chemistry of pentavalent uranium is an area of research that has enjoyed a recent explosion of activity and great strides have been made in the fundamental understanding of uranium(V) systems over the last few decades. With the benefit of hindsight, we see that uranium(V) is far more stable than previously thought; instead of being accessed by serendipity, uranium(V) complexes can now be synthesized using straightforward and predictable methods. Indeed, a large number of systems have been prepared and characterized, and definite themes are beginning to emerge. From a structural perspective, the complexes all contain flexible σ-/π-donor ligands that can act as a buffer to accommodate the needs of the uranium metal. The ability of these $N_{(amide)}$, $O_{(alkoxide)}$, $P_{(phosphine)}$, $S_{(thiolate)}$ and $C_{(carbocycle)}$ donors, along with even the uranyl and imido fragments, to adjust their electron-donating ability in response to the electronic demands of the uranium metal appears vital to the isolation and stability of the resultant pentavalent complexes.

And yet, even with all the synthetic advances made toward U^{V} systems over recent years, compared to the other uranium oxidation states (III, IV, VI), there is still so much that we do not understand about this enigmatic oxidation state. The dearth of available physical characterization data for molecular uranium(V) systems is a general problem in the field. This research area needs a better understanding of the 5f^{1} electronic structure and how it manifests itself physically and chemically through its influence on spectroscopic and thermodynamic properties. As seen from studies by our group and others, X-ray structural characterization alone is not sufficient. Over the past few decades a variety of techniques (^{1}H NMR spectroscopy, EPR spectroscopy, IR and Raman spectroscopy, cyclic voltammetry, UV-visible-NIR absorption spectroscopy, extended X-ray absorption fine stucture (EXAFS), variable-temperature magnetic susceptibility) have emerged as tools for probing electronic structure, bonding, speciation and metal-metal interactions. It is expected that further application of a combination of these techniques will greatly expand our understanding of uranium(V) systems in the future. Paired with sophisticated computational efforts, the data collected from these studies will provide important and necessary experimental benchmarks for achieving predictive tools for quantifying the chemical behavior and physical properties in these actinide systems.

Finally, understanding the nature of covalent bonding and through-bond communication between actinide metals in multimetallic networks also remains a computational and experimental challenge. As seen with the classic 5f^{1}-5f^{1} work by Andersen and Edelstein, and more recently by the groups of Mazzanti and Boncella, pentavalent uranium chemistry offers much to advance these aspects of actinide science. As such, future exploratory goals in the field should include the preparation of new types of multimetallic 5f^{1} compounds; we anticipate the appearance of new supporting ligands and bridging ligand platforms will help accomplish this objective.

Acknowledgements

For financial support of this work, we acknowledge Los Alamos National Laboratory (Director's Postdoctoral Fellowship to C.R.G.), the LANL G. T. Seaborg Institute for Transactinium Science (Postdoctoral Fellowship to C.R.G.), and the Division of Chemical Sciences, Office of Basic Energy Sciences, Heavy Element Chemistry program. The authors would also like to thank Drs. David E. Morris, P. Jeffrey Hay, Joe D. Thompson, Ping Yang, Thibault Cantat, David L. Clark, Anthony E. Vaughn, Eric J. Schelter, Robert K. Thomson (all LANL), Dr. Paul B. Duval (Shaw Areva MOX Services), Prof. Polly L. Arnold (Edinburgh), and Dr. Marinella Mazzanti (CEA-Grenoble) for stimulating discussions on the evolving field of pentavalent uranium over the past two years.

Notes and References

Los Alamos National Laboratory, Los Alamos, NM 87544, USA. Fax: 505-667-9905*; Tel:* 505-665-9553*; E-mail: kiplinger@lanl.gov*

† We have tried to be as comprehensive as possible herein; if any papers have been missed, please contact the authors and an addendum will be made available on the internet.

‡ During the preparation of this article, Arnold and Love published an overview on pentavalent uranyl complexes, which complements the present review. See: P. L. Arnold, J. B. Love and D. Patel, *Coord. Chem. Rev.* 2009, **XX**, #-#.

1 *The Chemistry of the Actinide and Transactinide Elements*, 3rd ed., L. R. Morss, N. M. Edelstein, J. Fuger, Eds.; Springer, Berlin, 2006, Vol. 1-5.

2 J. Selbin and J. D. Ortego, *Chem. Rev.*, 1969, **69**, 657-671.

3 G. Kniewald and M. Branica, *Mar. Chem.*, 1988, **24**, 1-12.

4 J. A. Fortner, A. J. Kropf, R. J. Finch, A. J. Bakel, M. C. Hash and D. B. Chamberlain, *J. Nucl. Mater.*, 2002, **304**, 56-62.

5 K. S. Finnie, Z. Zhang, E. R. Vance and M. L. Carter, *J. Nucl. Mater.*, 2003, **317**, 46-53.

6 K. Grossmann, T. Arnold, E. Krawczyk-Barsch, S. Diessner, A. Wobus, G. Bernhard and R. Krawietz, *Environ. Sci. Technol.*, 2007, **41**, 6498-6504.

7 E. S. Ilton, J.-F. Boily and P. S. Bagus, *Surf. Sci.*, 2007, **601**, 908-916.

8 J.-F. Boily and E. S. Ilton, *Surf. Sci.*, 2008, **602**, 3637-3646.

9 E. S. Ilton, A. Haiduc, C. L. Cahill and A. R. Felmy, *Inorg. Chem.*, 2005, **44**, 2986-2988.

10 J. C. Renshaw, L. J. C. Butchins, F. R. Livens, I. May, J. M. Charnock and J. R. Lloyd, *Environ. Sci. Technol.*, 2005, **39**, 5657-5660.

11 M. J. Wilkins, F. R. Livens, D. J. Vaughan and J. R. Lloyd, *Biogeochemistry*, 2006, **78**, 125-150.

12 D. E. Morris, *Inorg. Chem.*, 2002, **41**, 3542-3547.

13 G. Liu and J. V. Beitz, Optical Spectra and Electronic Structure. In *The Chemistry of the Actinide and Transactinide Elements*, 3rd ed., L. R. Morss, N. M. Edelstein, J. Fuger, Eds.; Springer, Berlin, 2006, Vol. 3., pp 2013-2111.

14 N. M. Edelstein and G. H. Lander, Magnetic Properties. In *The Chemistry of the Actinide and Transactinide Elements*, 3rd ed., L. R. Morss, N. M. Edelstein, J. Fuger, Eds.; Springer, Berlin, 2006, Vol. 4, pp 2225-2306.

15 N. Kaltsoyannis, P. J. Hay, J. Li, J. P. Blaudeau and B. E. Bursten, Theoretical Studies of the Electronic Structure of Compounds of the Actinide Elements. In *The Chemistry of the Actinide and Transactinide Elements*, 3rd ed., L. R. Morss, N. M. Edelstein, J. Fuger, Eds.; Springer, Berlin, 2006, Vol. 3, pp 1893-2012.

16 J. L. Ryan, *J. Inorg. Nucl. Chem.*, 1971, **33**, 153-177.

17 I. Grenthe, J. Drozdzynski, T. Fujino, E. C. Buck, T. E. Albrecht-Schmitt, and S. F. Wolf, Uranium. In *The Chemistry of the Actinide and Transactinide Elements*, 3rd ed.; L. R. Morss, N. M. Edelstein, J. Fuger, Eds.; Springer: The Netherlands, 2006; Vol 1, pp 253-698.

18 A. V. Soldatov, D. Lamoen, M. J. Konstantinovic, S. Van den Berghe, A. C. Scheinost and M. Verwerft, *J. Solid State Chem.*, 2007, **180**, 54-61.

19 N. Belai, M. Frisch, E. S. Ilton, B. Ravel and C. L. Cahill, *Inorg. Chem.*, 2008, **47**, 10135-10140.

20 H. G. Heal, *Trans. Faraday Soc.*, 1949, **45**, 1-11.

21 H. G. Heal and J. G. N. Thomas, *Trans. Faraday Soc.*, 1949, **45**, 11-20.

22 B. McDuffie and C. N. Reilley, *Anal. Chem.*, 1966, **38**, 1881-1887.

23 A. Ekstrom, *Inorg. Chem.*, 1974, **13**, 2237-2241.

24 H. Steele and R. J. Taylor, *Inorg. Chem.*, 2007, **46**, 6311-6318.

25 C. Miyake, Y. Yamana, S. Imoto and H. Ohya-Nishiguchi, *Inorg. Chim. Acta*, 1984, **95**, 17-21.

26 C. Miyake, T. Kondo, S. Imoto and H. Oya-Nishiguchi, *J. Less-Common Met.*, 1986, **122**, 313-317.

27 K. Mizuguchi, Y. Y. Park, H. Tomiyasu and Y. Ikeda, *J. Nucl. Sci. Technol.*, 1993, **30**, 542-548.

28 K. Mizuoka, I. Grenthe and Y. Ikeda, *Inorg. Chem.*, 2005, **44**, 4472-4474.

29 S.-H. Lee, K. Mizuguchi, H. Tomiyasu and Y. Ikeda, *J. Nucl. Sci. Technol.*, 1996, **33**, 190-192.

30 S.-Y. Kim, T. Asakura, Y. Morita, G. Uchiyama and Y. Ikeda, *Radiochim. Acta*, 2005, **93**, 75-81.

31 K. Mizuoka, S.-Y. Kim, M. Hasegawa, T. Hoshi, G. Uchiyama and Y. Ikeda, *Inorg. Chem.*, 2003, **42**, 1031-1038.

32 K. Mizuoka, S. Tsushima, M. Hasegawa, T. Hoshi and Y. Ikeda, *Inorg. Chem.*, 2005, **44**, 6211-6218.

33 K. Mizuoka and Y. Ikeda, *Inorg. Chem.*, 2003, **42**, 3396-3398.

34 J.-C. Berthet, M. Nierlich and M. Ephritikhine, *Angew. Chem., Int. Ed.*, 2003, **42**, 1952-1954.

35 P. J. Hay, R. L. Martin and G. Schreckenbach, *J. Phys. Chem. A.*, 2000, **104**, 6259-6270.

36 T. I. Docrat, J. F. W. Mosselmans, J. M. Charnock, M. W. Whiteley, D. Collison, F. R. Livens, C. Jones and M. J. Edmiston, *Inorg. Chem.*, 1999, **38**, 1879-1882.

37 T. W. Hayton and G. Wu, *J. Am. Chem. Soc.*, 2008, **130**, 2005-2014.

38 T. W. Hayton and G. Wu, *Inorg. Chem.*, 2008, **47**, 7415-7423.

39 P. L. Arnold, D. Patel, C. Wilson and J. B. Love, *Nature*, 2008, **451**, 315-317.

40 J. J. Berard, G. Schreckenbach, P. L. Arnold, D. Patel and J. B. Love, *Inorg. Chem.*, 2008, **47**, 11583-11592.

41 G. Zi, L. Jia, E. L. Werkema, M. D. Walter, J. P. Gottfriedsen and R. A. Andersen, *Organometallics*, 2005, **24**, 4251-4264.

42 J.-C. Berthet, G. Siffredi, P. Thuery and M. Ephritikhine, *Chem. Commun.*, 2006, 3184-3186.

43 L. Natrajan, F. Burdet, J. Pecaut and M. Mazzanti, *J. Am. Chem. Soc.*, 2006, **128**, 7152-7153.

44 G. Nocton, P. Horeglad, J. Pecaut and M. Mazzanti, *J. Am. Chem. Soc.*, 2008, **130**, 16633-16645.

45 E. A. Boudreaux, L. N. Mulay, *Theory and Applications of Molecular Paramagnetism*; Wiley: New York, 1976, p. 512.

46 F. Burdet, J. Pecaut and M. Mazzanti, *J. Am. Chem. Soc.*, 2006, **128**, 16512-16513.

47 L. P. Spencer, E. J. Schelter, P. Yang, R. L. Gdula, B. L. Scott, J. D. Thompson, J. L. Kiplinger, E. R. Batista, J. M. Boncella, *Angew. Chem., Int. Ed.* 2008, In Press.

48 P. G. Eller and P. J. Vergamini, *Inorg. Chem.*, 1983, **22**, 3184-3189.

49 F. A. Cotton, D. O. Marler and W. Schwotzer, *Inorg. Chem.*, 1984, **23**, 4211-4115.

50 F. A. Cotton, D. O. Marler and W. Schwotzer, *Inorg. Chim. Acta*, 1984, **85**, L31-L32.

51 R. H. Cayton, K. J. Novo-Gradac and B. E. Bursten, *Inorg. Chem.*, 1991, **30**, 2265-2272.

52 R. A. Andersen, *Inorg. Chem.*, 1979, **18**, 1507-1509.

53 A. Zalkin, J. G. Brennan and R. A. Andersen, *Acta Crystallogr.*, 1988, **C44**, 1553-1554.

54 P. Roussel, R. Boaretto, A. J. Kingsley, N. W. Alcock and P. Scott, *J. Chem. Soc., Dalton Trans.*, 2002, 1423-1428.

55 I. Castro-Rodriguez, K. Olsen, P. Gantzel and K. Meyer, *J. Am. Chem. Soc.*, 2003, **125**, 4565-4571.

56 R. D. Shannon, *Acta Crystallogr., Sect. A*, 1976, **A32**, 751-767.

57 I. Castro-Rodriguez, H. Nakai and K. Meyer, *Angew. Chem., Int. Ed.*, 2006, **45**, 2389-2392.

58 S. C. Bart, C. Anthon, F. W. Heinemann, E. Bill, N. M. Edelstein and K. Meyer, *J. Am. Chem. Soc.*, 2008, **130**, 12536-12546.

59 K. Meyer, D. J. Mindiola, T. A. Baker, W. M. Davis and C. C. Cummins, *Angew. Chem., Int. Ed.*, 2000, **39**, 3063-3066.

60 J. Selbin, C. J. Ballhausen and D. G. Durrett, *Inorg. Chem.*, 1972, **11**, 510-515.

61 D. Gourier, D. Caurant, T. Arliguie and M. Ephritikhine, *J. Am. Chem. Soc.*, 1998, **120**, 6084-6092.

62 M. Wedler, M. Noltemeyer and F. T. Edelmann, *Angew. Chem., Int. Ed.*, 1992, **31**, 72-73.

63 S. J. Coles, P. G. Edwards, M. B. Hursthouse and P. W. Read, *J. Chem. Soc., Chem. Commun.*, 1994, 1967-1968.

64 S. J. Coles, A. A. Danopoulos, P. G. Edwards, M. B. Hursthouse and P. W. Read, *J. Chem. Soc., Dalton Trans.*, 1995, 3401-3408.

65 L. Salmon, P. Thuery, S. Miyamoto, T. Yamato and M. Ephritikhine, *Polyhedron*, 2006, **25**, 2439-2446.

66 L. Salmon, P. Thuery and M. Ephritikhine, *Eur. J. Inorg. Chem.*, 2006, 4289-4293.

67 P. C. Leverd and M. Nierlich, *Eur. J. Inorg. Chem.*, 2000, 1733-1738.

68 P. Roussel, P. B. Hitchcock, N. D. Tinker and P. Scott, *Inorg. Chem.*, 1997, **36**, 5716-5721.

69 L. Salmon, P. Thuery and M. Ephritikhine, *Polyhedron*, 2007, **26**, 631-636.

70 J. C. Berthet and M. Ephritikhine, *J. Chem. Soc., Chem. Commun.*, 1993, 1566-1567.

71 S. Fortier, G. Wu and T. W. Hayton, *Inorg. Chem.*, 2008, **47**, 4752-4761.

72 E. R. Sigurdson and G. Wilkinson, *J. Chem. Soc., Dalton Trans.*, 1977, 812-818.

73 T. Arliguie, M. Lance, M. Nierlich, J. Vigner and M. Ephritikhine, *J. Chem. Soc., Chem. Commun.*, 1995, 183-184.

74 J. Li and B. E. Bursten, *J. Am. Chem. Soc.*, 1997, **119**, 9021-9032.

75 P. B. Duval, C. J. Burns, D. L. Clark, D. E. Morris, B. L. Scott, J. D. Thompson, E. L. Werkema, L. Jia and R. A. Andersen, *Angew. Chem., Int. Ed.*, 2001, **40**, 3357-3361.

76 J. Maynadie, N. Barros, J.-C. Berthet, P. Thuery, L. Maron and M. Ephritikhine, *Angew. Chem., Int. Ed.*, 2007, **46**, 2010-2012.

77 J. G. Brennan and R. A. Andersen, *J. Am. Chem. Soc.*, 1985, **107**, 514-516.

78 R. K. Rosen, R. A. Andersen and N. M. Edelstein, *J. Am. Chem. Soc.*, 1990, **112**, 4588-4590.

79 P. C. Blake, M. F. Lappert, R. G. Taylor, J. L. Atwood and H. Zhang, *Inorg. Chim. Acta*, 1987, **139**, 13-20.

80 D. S. J. Arney and C. J. Burns, *J. Am. Chem. Soc.*, 1993, **115**, 9840-9841.

81 J. C. Berthet and M. Ephritikhine, *Coord. Chem. Rev.*, 1998, **178-180**, 83-116.

82 M. Ephritikhine, J. C. Berthet, C. Boisson, M. Lance and M. Nierlich, *J. Alloys Compd.*, 1998, **271-273**, 144-149.

83 C. Boisson, J.-C. Berthet, M. Lance, M. Nierlich, J. Vigner and M. Ephritikhine, *J. Chem. Soc., Chem. Commun.*, 1995, 543-544.

84 C. Boisson, J.-C. Berthet, M. Lance, J. Vigner, M. Nierlich and M. Ephritikhine, *J. Chem. Soc., Dalton Trans.*, 1996, 947-953.

85 C. Den Auwer, C. Madic, J. C. Berthet, M. Ephritikhine, J. J. Rehr and R. Guillaumont, *Radiochim. Acta*, 1997, **76**, 211-218.

86 D. Gourier, D. Caurant, J. C. Berthet, C. Boisson and M. Ephritikhine, *Inorg. Chem.*, 1997, **36**, 5931-5936.

87 T. Arliguie, M. Fourmigue and M. Ephritikhine, *Organometallics*, 2000, **19**, 109-111.

88 L. Belkhiri, T. Arliguie, P. Thuery, M. Fourmigue, A. Boucekkine and M. Ephritikhine, *Organometallics*, 2006, **25**, 2782-2795.

89 C. R. Graves, B. L. Scott, D. E. Morris and J. L. Kiplinger, *J. Am. Chem. Soc.*, 2007, **129**, 11914-11915.

90 C. R. Graves, P. Yang, S. A. Kozimor, A. E. Vaughn, D. L. Clark, S. D. Conradson, E. J. Schelter, B. L. Scott, J. D. Thompson, P. J. Hay, D. E. Morris and J. L. Kiplinger, *J. Am. Chem. Soc.*, 2008, **130**, 5272-5285.

91 C. R. Graves, A. E. Vaughn, E. J. Schelter, B. L. Scott, J. D. Thompson, D. E. Morris and J. L. Kiplinger, *Inorg. Chem.*, 2008, **47**, 11879-11891.

92 C. R. Graves, B. L. Scott, D. E. Morris and J. L. Kiplinger, *Organometallics*, 2008, **27**, 3335-3337.

93 C. R. Graves, B. L. Scott, D. E. Morris and J. L. Kiplinger, *Chem. Commun.*, 2008, 776-778.

94 D. S. Williams and A. V. Korolev, *Inorg. Chem.*, 1998, **37**, 3809-3819.

95 R. A. Penneman, G. D. Sturgeon and L. B. Asprey, *Inorg. Chem.*, 1964, **3**, 126-129.

96 M. J. Reisfeld and G. A. Crosby, *Inorg. Chem.*, 1965, **4**, 65-70.

97 N. Edelstein, D. Brown and B. Whittaker, *Inorg. Chem.*, 1974, **13**, 563-567.